MAGNETIC RELAXATION AND RESONANCE PHENOMENA IN FERRITES

BY

H. P. J. WIJN

1953

DRUKKERIJ v/h KEMINK EN ZOON N.V. - DOMPLEIN 2 - UTRECHT

MAGNETIC RELAXATION AND RESONANCE PHENOMENA IN FERRITES

MAGNETIC RELAXATION AND RESONANCE PHENOMENA IN FERRITES

PROEFSCHRIFT

TER VERKRIJGING VAN DE GRAAD VAN DOCTOR IN DE WIS- EN NATUURKUNDE AAN DE RIJKSUNIVERSITEIT TE LEIDEN, OP GEZAG VAN DE RECTOR MAGNIFICUS Dr J. J. L. DUYVENDAK, HOOGLERAAR IN DE FACULTEIT DER LETTEREN EN WIJSBEGEERTE, PUBLIEK TE VERDEDIGEN OP WOENSDAG 28 JANUARI 1953 TE 16 UUR

DOOR

HENRICUS PETRUS JOHANNES WIJN

GEBOREN TE EINDHOVEN IN 1922

1953

DRUKKERIJ EN UITGEVERS-MAATSCHAPPIJ v/h KEMINK EN ZOON N.V.
DOMPLEIN 2 — UTRECHT

Promotor:
Prof. Dr H. B. G. CASIMIR

Aan mijn VADER

CONTENTS

GENERAL INTRODUCTION

The use of ferromagnetic materials was restricted for a long time to the range of low frequencies, as rapid changes in the magnetic flux cause large eddy-current losses in the metallic ferromagnetic materials. A decrease of these losses could be obtained by using laminated cores and dust cores. A large step forward was made by S n o e k in developing the ferrites to technically useful materials. These ferrites are ferromagnetic oxides with an electric resistivity that can be varied between 10^{-2} and 10^{7} Ohmcm, so that in most cases eddy currents may be neglected up to the highest frequencies.

We have investigated the magnetization processes which take place when a ferrite is magnetized both in weak and strong magnetic fields. Therefore the magnetization curves of ferrites with widely varying physical and chemical properties, have been measured as a function of frequency.

The decrease of the initial permeability of ferrites at high frequencies and the attendant increase of the losses have been related by S n o e k to a ferromagnetic resonance of the electron spins. This implies the assumption that the initial permeability of ferrites is caused by a rotation in unison of the spins in each W e i s s domain, which assumption is at variance with the known fact that in ferromagnetic metals the initial permeability is mainly a consequence of reversible domain-wall displacements. Therefore we have measured the *spectrum* of μ_0 in a wide frequency range for several ferrites, and especially for a ferrite under such conditions that merely rotations in unison of the spins in the W e i s s domains can contribute to the permeability. It is also known that in weak magnetic fields at low frequencies residual losses are found in ferrites. However, the origin of these losses is obscure. In this thesis some measurements will be dealt with that can shed some light on the nature of these losses.

The irreversible domain-wall displacements in ferromagnetic materials are a cause of the hysteresis losses; they are also at least in part responsible for the distortion brought about by such coil cores in electric circuits. In iron at high frequency these irreversible wall-displacements do not occur. This might be caused by a damping by micro eddy-currents or by an inertia corresponding to an equivalent mass that can be ascribed to a moving wall. Therefore it is important to investigate whether in ferrites with a high resistivity this type of wall displacement also shows a relaxation at high frequency. In order to do this an apparatus has been developed allowing the measurement of the magnetization curve and distortion characteristics of ferrites from low frequency up to 1.5 Mc/s. The results of the measurements of different ferrites will be discussed.

1. FERRITES

1. 1. *Crystal structure and physical properties of ferrites.*

The chemical composition of ferrites is in most cases given by the formula $MeFe_2O_4$, in which Fe denotes the ferric ion and Me a bivalent metal ion or a combination of bivalent metal ions. All ferrites studied in this thesis have the crystal structure of the mineral spinel, *i.e.* the face centred cubic packing of oxygen ions given in figure 1. Two kinds of interstices can be distinguished in this structure, the so-called tetrahedral and octahedral holes which are surrounded by 4 and 6 oxygen ions respectively. For 32 oxygen ions in the unit cell 16 octahedral and 8 tetrahedral sites are occupied by metal ions having an ion diameter between 0.6 and 0.9 Å, *e.g.* Ni^{2+}, Mg^{2+}, Zn^{2+}, Fe^{2+} and Fe^{3+} ions. The crystal structure of the spinel $MgAl_2O_4$ was first reported by W. H. Bragg (1). Barth and Posnjak (2) and also Verwey and Heilmann (3) investigated the distribution of the ions over the available positions. The latter came to the conclusion that zinc and cadmium ferrite have the normal spinel structure, *i.e.* the bivalent metal ions occupy the tetrahedral positions and all ferric ions occupy octahedral positions. All other known ferrites are so-called inverse spinels. In this inverted structure the tetrahedral positions are occupied by ferric ions and the rest of the ferric ions together with the bivalent ions are distributed over the octahedral positions, either ordered or at random. Recently intermediate forms were found for magnesium and copper ferrite (4).

The ferrites we have used are mostly homogeneous mixed crystals of zinc ferrite with another single ferrite. In this case the tetrahedral positions are occupied by all or almost all the zinc ions completed by ferric ions. The rest of the ions are in the octahedral positions. Formula [1] gives schematically a ferrite with the chemical composition in mol % 23 MnO, 27 ZnO and 50 Fe_2O_3:

$$\overleftarrow{\qquad}\qquad\overrightarrow{\qquad} \\ Zn_{0.54}\ Fe^{3+}_{0.46}\quad [Mn_{0.46}\ Fe^{3+}_{1.54}]\ O_4\ , \qquad [1]$$

where the occupation of the tetrahedral positions is given before

the brackets and that of the octahedral positions within the brackets.

According to Néel (5) the ferromagnetism in ferrites is caused by an anti-parallel orientation of the magnetic moments of the ions in the octahedral and tetrahedral positions. As Kramers (6) has already indicated this anti-parallel orientation can be caused by the indirect exchange energy between magnetic ions separated by an oxygen ion (7). From the paramagnetic and ferromagnetic behaviour of some ferrites Néel (5) derives a strong negative tetrahedral-octahedral and a small negative tetrahedral-tetrahedral exchange, and also a small octahedral-octahedral exchange, which might be positive or negative.

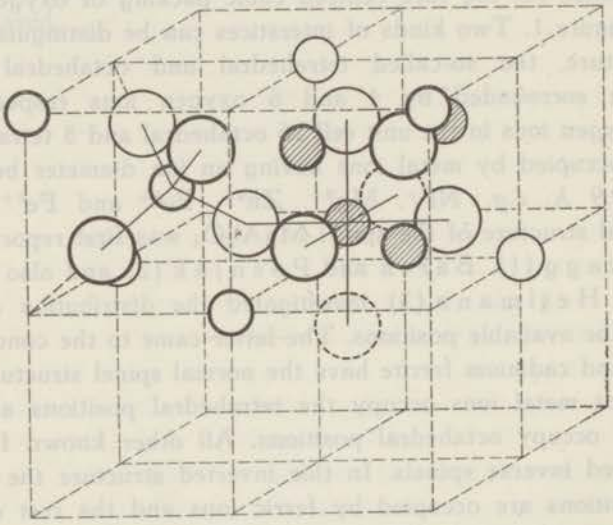

Fig. 1. Unit cell of spinel structure. The large spheres represent the oxygen ions. The small white and hatched spheres represent the metal ions in the tetrahedral and octahedral positions respectively.

The relatively small saturation magnetization of ferrites can be explained by Néel's hypothesis of anti-parallel orientation of magnetic spins which has been indicated by the arrows in [1]. A comparison of the saturation magnetization of single ferrites as predicted by Néel's theory with those which have been found experimentally is given by Néel (8) and Gorter (9). Extensive experiments by Gorter (9) and Guillaud (10) on various

mixed ferrites confirm the strong anti-parallel orientation of the spins in different lattice positions and the weak tendency to anti-parallel orientation of the spins of the ions in octahedral lattice positions. This latter tendency can prevent the complete anti-parallel orientation of the spins in tetrahedral and octahedral positions. Neutron diffraction experiments (11, 12) with Fe_3O_4 and $NiFe_2O_4$ proved that both Verwey's picture on the ion distribution and Néel's picture on the anti-parallel spin orientation in ferrites are correct in these instances.

Two important properties of the ferrites are the initial permeability which may be higher than 1000, and the electrical conductivity which is at least 10^6 times smaller than that found for metals.

Snoek (13) showed already that it is possible to obtain high values for the initial permeability in the case of mixed ferrites having a Curie point not far above room temperature. In a binary system of homogeneous mixed crystals of ferrites the Curie point is intermediate between those of the single ferrites under consideration. For instance, a Curie point θ_c of about 200° C is obtained for mixed crystals of nickel ferrite ($\theta_c = 585°$ C) with zinc ferrite (whether zinc ferrite is paramagnetic or ferromagnetic with a very low Curie point cannot be said with certainty) if the molar composition is chosen as 18 NiO, 32 ZnO and 50 Fe_2O_3 (see figure 2; θ_c is defined as the temperature at which the saturation magnetization I_s becomes zero). The highest initial permeability is found at a temperature somewhat below the Curie point, which means that the crystal anisotropy decreases more with increasing temperature than I_s^2 does. By lowering the Curie point along these lines Snoek (13) obtained for the above mentioned nickel zinc ferrite an initial permeability μ_o of 800 at room temperature. Figure 2 gives the dependence of μ_o on temperature for this nickel zinc ferrite.

The initial permeability is also dependent on the saturation magnetostriction λ_s, *i.e.* the relative change in length of the magnetic material when, starting from the demagnetized state, it is magnetized to saturation. In a ferrite having an average internal stress σ_i the stress anisotropy is determined by the product $\lambda_s \cdot \sigma_i$.

Ferrites with a high initial permeability should possess a very small λ_s. Apart from Fe_3O_4 ($\lambda_s = + 40 \cdot 10^{-6}$) all known ferrites have a negative magnetostriction at room temperature. Went (see reference (13)) has found that λ_s of ferrites becomes very small and can even vanish in homogeneous mixed crystals containing Fe_3O_4 as

one of the components. Thus by preparing a ferrite containing ferrous ions the initial permeability can increase but at the same time its resistivity decreases as will be shown below, and it will depend entirely on the application of the ferrite whether a small content of ferrous ions is favourable or not.

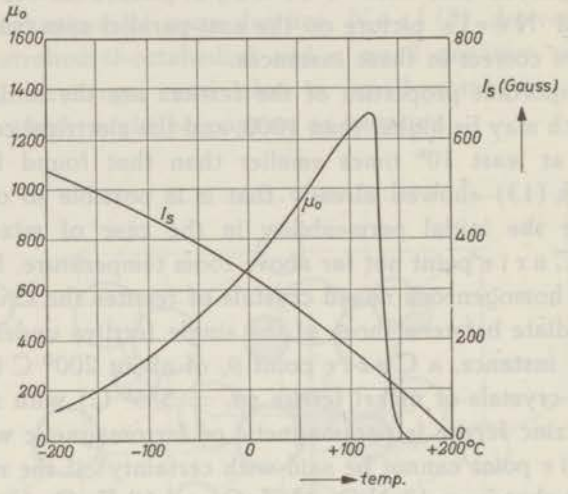

Fig. 2. Temperature dependence of μ_0 and I_s for a nickel zinc ferrite having the molar composition 18 NiO, 32 ZnO and 50 Fe_2O_3.

The electric conductivity of oxides is primarily determined by the presence of ions of the same metal but having different electric charges, if these ions are distributed over crystallografic equivalent positions. According to de Boer and Verwey (14) the small resistivity of magnetite, $\varrho = 10^{-2}$ Ohmcm at room temperature, is to be ascribed to the exchange of electrons between ferric and ferrous ions in equal lattice positions. If ferrites, for which the stoechiometric composition does not contain ferrous ions, are fired in an insufficiently oxidizing atmosphere (see chapter 1.2), a certain amount of the ferric ions will be reduced to ferrous ions and consequently the material will have a low resistivity (15). On the other hand ferrites containing no ferrous ions for instance stoechiometrical nickel ferrite, show a high resistivity, $\varrho > 10^7$ Ohmcm.

1.2. *Method of preparation of the ferrites to be examined.*

Part of the ferrites used in this investigation have been prepared by E. W. Gorter and part of them are the commercially available Philips Ferroxcube materials.

All the ferrites examined have been obtained by a sintering process. In order to obtain a good homogeneous product a mixture of the composing oxides (or other compounds) is thoroughly mixed and ground under alcohol in an iron ball mill. After drying, this mixture is prefired for several hours at 800 to 1000° C in air, so as to obtain a decomposition of the compounds into oxides and to achieve a more or less complete reaction of the oxides. This product is pulverized in turn and homogenized by prolonged grinding in the same ball mill. When the powder is dried again, a binder is added (mostly water, 5% by volume) and a ring is pressed with a pressure of 1½ tons/cm². Finally these rings are sintered at 1200 tot 1300° C in the gastight ceramic tube of a molybdenum furnace. The oxygen content of the atmosphere is controlled so that the desired ratio of ferric and ferrous ions is obtained. The furnace is heated up for about three hours, after which it remains for two hours at the higher temperature, and is then allowed to cool down to room temperature in about five hours. The final product is a ceramic with a porosity between 5% and 25%, depending on the chemical composition of the ferrites, the reactivity of the raw material, the sintering temperature and the method of grinding.

2. MEASURING PROCEDURE

2. 1. *Introduction.*

In the preceding chapter the saturation magnetization I_s of a ferrite is discussed in connection with its chemical composition. It appeared that I_s depends on the distribution of the magnetic ions over the different crystal lattice positions. In the following, this atomic picture will be abandoned and we wish to examine what types of magnetization processes take place when a ferrite is magnetized. For this reason we have measured as a function of frequency the relation between the applied magnetic field strength and the induction which it brings about. The involved losses have also been determined. Dependent on the range of field strengths chosen, the methods of measurement can be divided into two kinds. For very small field strengths (*i.e.* field strengths at which the induction in the ferrite is less than 1 Gauss) a general survey of the different measuring methods is given by v. d. Burgt, Gevers and Wijn (16).

In discussing results which have been obtained by using these methods, the original literature will be quoted. In this chapter we describe the methods for measuring some properties of ferrites at high induction, namely the magnetization curve and the distortion. The method for measuring the total losses will be described in chapter 8. 2.

2. 2. *The magnetization curve.*

Definition. We demagnetize the ferrites before measuring, by applying a slowly varying magnetic field (50 c/s) whose amplitude is gradually reduced to zero avoiding any fluctuation. The directions of this field and the measuring field are the same. Starting from this condition of the ferrite, three curves can be defined, which give a relation between the induction and the field strength in the ferromagnetic material:

a. *The normal magnetization curve.* With a ballistic galvanometer the increase of the induction of the ferrite is measured when

the magnetic field is increased by steps (see *e.g.* Gumlich (17) page 58).

b. *The commutation curve.* The applied magnetic field is commutated and the resultant induction change in the ferrite is measured. This is taken to be twice the induction corresponding to the commutated field strength. The relation which is found between the field strength and the induction if the measurements are carried out in a sequence of increasing field strength is called the commutation curve (see reference (17) page 60).

c. *The alternating current magnetization curve* *). A sinusoidal magnetic field in a ferrite core generally gives rise to a non-sinusoidally varying induction. The single-valued function which gives the relation between the amplitude H_{max} of the magnetic field and the maximum value of the induction B_{max} in the ferrite core will be called the magnetization curve of the ferrite at the frequency of the field H. This definition is only useful for ferromagnetic materials with a high resistivity, for otherwise the magnetization curve is highly influenced by eddy currents which depend on the dimensions of the sample. In the following we will be mainly concerned with this magnetization curve.

Method of measuring the magnetization curve. In order to avoid external demagnetizing effects the magnetization curve is always measured on annular ferrite cores (with rectangular cross section).

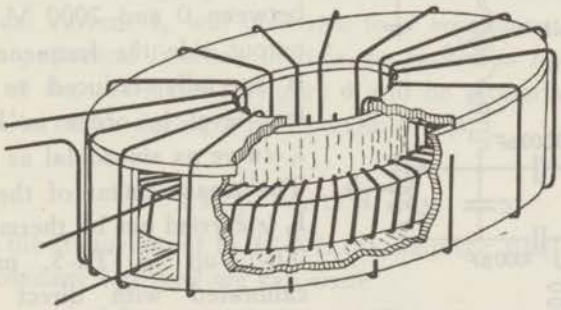

Fig. 3. Ferrite transformer used for the measurement of the magnetization curve.

Average dimensions of these cores are: outer and inner diameter 30 and 20 mm respectively, and a height varying between 0.5 and 5 mm. The latter choice depends on the measuring frequency as

*) If there is no danger of ambiguity in the following the adjective "alternating current" will be omitted.

will be explained later. This ferrite ring is put as a core in a transformer circuit. The primary of this circuit is wound tightly on the core, the secondary is separated from the primary by a polythene case in order to avoid too large a capacity between both, see figure 3. A diagram of the measuring circuit is given in figure 4. T is the transformer with primary and secondary coils L_p and L_s. A Hartley-type oscillator of 200 Watt supplies a primary current I_p having a low amount of higher harmonics. The frequency of this oscillator can be varied between 56 and 1800 Kc/s by tapping the coil L and by connecting capacities C, see figure 5.

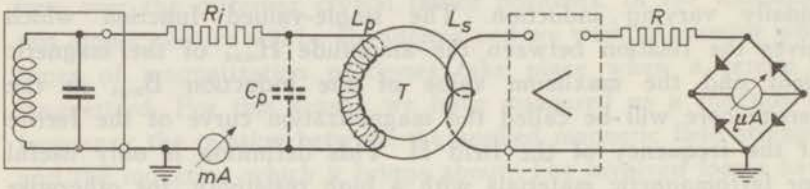

Fig. 4. Circuit for measuring the magnetization curve. The amplifier used at low frequency is represented by dotted lines.

The voltage on the oscillator circuit and consequently the current I_p is adjusted by the voltage on the anode of the transmission valve. This latter voltage is taken from a rectifier, the output of which can be regulated continuously between 0 and 2000 V. On the output side the frequency factor is specially reduced to a very low level in order to keep the I_p-curve as sinusoidal as possible. The measurement of the current I_p is carried out by thermocouples Th-1 up to Th-5, previously calibrated with direct current. The measuring ranges of these couples extend from 1 to 200 mA and this calibration is independent of frequency up to 1800 Kc/s because of their small RC-time ($C \leq 2$ pF and $R \leq 70$ Ohm).

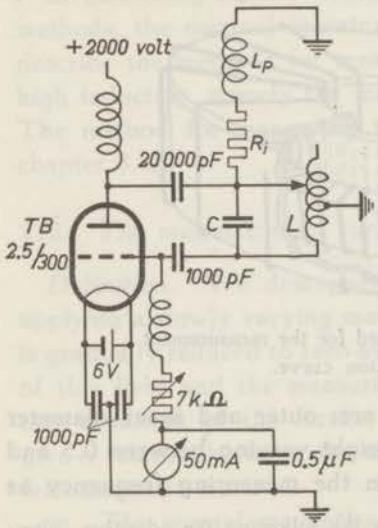

Fig. 5. The Hartley-type oscillator.

The relation between the effective value of the sinusoidal current I_p and the maximum magnetic field strength H_{max} in the annular ferrite core is given by the formula

$$H_{max} = \frac{0.4\, I_p\, n_p\, \sqrt{2}}{d_{av}}, \qquad [2]$$

where n_p is the number of turns of the primary L_1 and $d_{av} = \frac{d_o + d_i}{2}$ is the average of the outer and inner diameter of the core *).

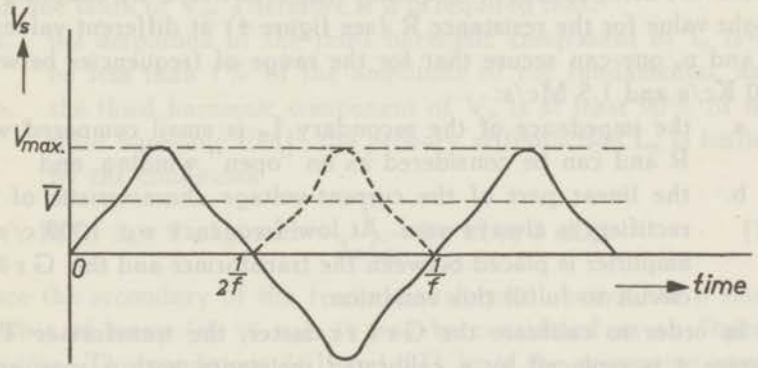

Fig. 6. Secondary voltage V_s of the transformer T.

The maximum induction B_{max} in the ferrite core is measured with a full-wave rectifying Grätz-circuit as given in figure 4. A sinusoidal current I_p will give rise to a secondary voltage V_s which is a periodical function of time, as shown in figure 6. The deflection of the μA-meter in figure 4 will be proportional to the average value of V_s during a half period:

$$\overline{V} = 2f \int_0^{\frac{1}{2f}} V_s(t)\, dt, \qquad [3]$$

where f is the frequency of H. If Φ is the magnetic flux surrounded by the secondary coil then we can write

$$V_s(t) = -\frac{d\Phi}{dt} \cdot 10^{-8} = -n_s S \frac{dB}{dt} \cdot 10^{-8}\ \text{Volt}, \qquad [4]$$

where B is the magnetic induction, S the cross section of the core

*) The diameters d_o and d_i differ at most 16% from d_{av}. Therefore the value of H_{max} depends on the place in the core, and a mean value of B_{max} is measured. It will appear from the measuring results that the error in the measured magnetization curve is small.

and n_s the number of turns of the secondary of the transformer. Substitution of equation [4] in [3] followed by the integration over half of a period gives a relation between the maximum induction B_{max} in the ferrite core and the average voltage $\overline{V}$ read from the Grätz meter:

$$B_{max} = \frac{\overline{V} \cdot 10^8}{4\, n_s\, f\, S} \text{ Gauss.} \qquad [5]$$

The characteristics of the four germanium rectifiers of the Grätz meter are independent of frequency below 10 Mc/s. By choosing the right value for the resistance R (see figure 4) at different values of f and n_s one can secure that for the range of frequencies between 50 Kc/s and 1.5 Mc/s:

a. the impedance of the secondary L_s is small compared with R and can be considered as an "open" winding, and
b. the linear part of the current-voltage characteristic of the rectifiers is always used. At low frequency *e.g.* 1000 c/s an amplifier is placed between the transformer and the Grätz circuit to fulfill this condition.

In order to calibrate the Grätz meter, the transformer T of figure 4 is replaced by a calibrated resistance with a very small time constant ($< 10^{-8}$). A sinusoidal current through this resistance is measured by one of the thermocouples. The known value of this current permits one to calculate the effective voltage V which corresponds to a certain deflection of the μA-meter. These calibrations differ by a small percentage for the various frequencies used on account of the selfcapacity of the resistance R and the capacity between the μA-meter and earth. This method of calibrating has the additional advantage that the measurement of the field strength and the induction depends on the same direct current meter and thermocouples so that errors in their calibration have only a small influence on the measured magnetization curve.

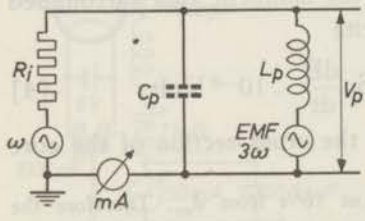

Fig. 7. Equivalent circuit for the primary of the transformer.

Limitations to the range in which the magnetization curve can be measured. Since there is always a selfcapacity C_p between the terminals of the coil L_p, the current I_p read from the mA-meter in figure 4 is smaller than the current through the coil L_p.

If it is required that at the circular frequency ω, the current reading deviates less than 1% from the true value, the limitation of the selfinduction L_p of the primary is given by

$$\omega^2 L_p C_p \leqslant 10^{-2}. \qquad [6]$$

The primary current I_p will be distorted as a result of the non-linearity of the magnetization curve of the ferrite. Schematically an EMF of the third harmonic can be placed in series with L_p, see figure 7. In most cases (see chapter 3. 1) this EMF is smaller than one tenth of V_p. Therefore if it is required that:

a. the amplitude of the third harmonic component of I_p is to be less than 1% of the amplitude of the fundamental, and
b. the third harmonic component of V_p is at least 90% of the third harmonic EMF, the primary selfinduction L_p is limited by the conditions

$$R_i \geqslant 3 \times 3\ \omega L_p \text{ and } \frac{1}{3\omega C_p} \geqslant 13 \times 3\ \omega L_p. \qquad [7]$$

Since the secondary of the ferrite transformer always has a small number of turns ($n_s < n_p$), it may be considered as an "open" winding. The conditions [6] and [7] limit the measuring range since for a fixed frequency and self capacitance the selfinduction of the primary coil is limited. This implies a limitation for n_p. Moreover the maximum primary current I_p from the oscillator is 200 mA, so that the maximum magnetic field strength is fixed. If measurements have to be carried out at still higher field strengths and frequencies, the ferrite core can be ground to a thickness of about 0.5 mm so as to reduce L_p. In these cases however, it will be difficult to obtain reliable results on account of the large amount of heat generated in the core.

2. 3. *Definition and method of measuring the non-linear behaviour of ferrites.*

Definition. A sinusoidal current of frequency f passing through the primary of the ferrite transformer T (figure 4) will induce in the secondary a voltage which is a periodical function of time. This voltage can be analysed into a Fourier series having the fundamental frequency f and higher harmonics. The distortion is caused bij the non-linear relationship between the magnetic field strength and the induction in the ferrite core. Usually the distortion

D caused bij the core material in a transformer circuit is given by the formula

$$D = \sqrt{\frac{\sum_{n=1}^{\infty} V_n^2}{V_o^2}} . \qquad [8]$$

V_n denotes the amplitude of the n-th harmonic of the secondary voltage V_s. We will define the distortion of a core material as the ratio of the amplitudes of the third harmonic and the fundamental of the secondary voltage of an open transformer completely filled with this core material, when the primary current is sinusoidal. This definition is permissible since the magnetization curve and the hysteresis loop are symmetrical with respect to the origin ($H = 0$, $B = 0$) so that only uneven harmonics occur. Moreover it will appear that the amplitudes of the fifth and higher harmonics are smaller than one-tenth of the amplitude of the third harmonic and as a function of frequency these higher harmonics behave in an analogous way as the third harmonic.

Method of measuring the third harmonic. The analysis of the secondary voltage V_s is carried out with a selective voltmeter, which has been made in co-operation with Dr J. J. Zaalberg van Zelst. Figure 8 shows its block diagram and the details of the circuit are given in figure 9. A standard oscillator with amplifier

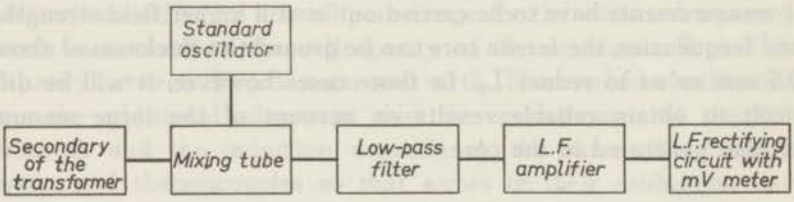

Fig. 8. Block diagram of the selective voltmeter.

gives a sinusoidal voltage to the third grid of a mixing tube ECH 21. The frequency of the signal can be matched with that of the fundamental or with one of the higher harmonics of the secondary voltage of the measuring transformer. The latter voltage is applied to the first grid of the mixing tube. The voltage of the third grid of the tube ECH 21 must be 8 Volts and may not vary with frequency in order to have a frequency-independent amplification

factor. This voltage therefore is checked by a mA-meter which measures the current between this grid and earth. The low frequency mixed signal passes through a low-pass filter and a low-frequency amplifier and is finally measured with a cuprox voltmeter *).

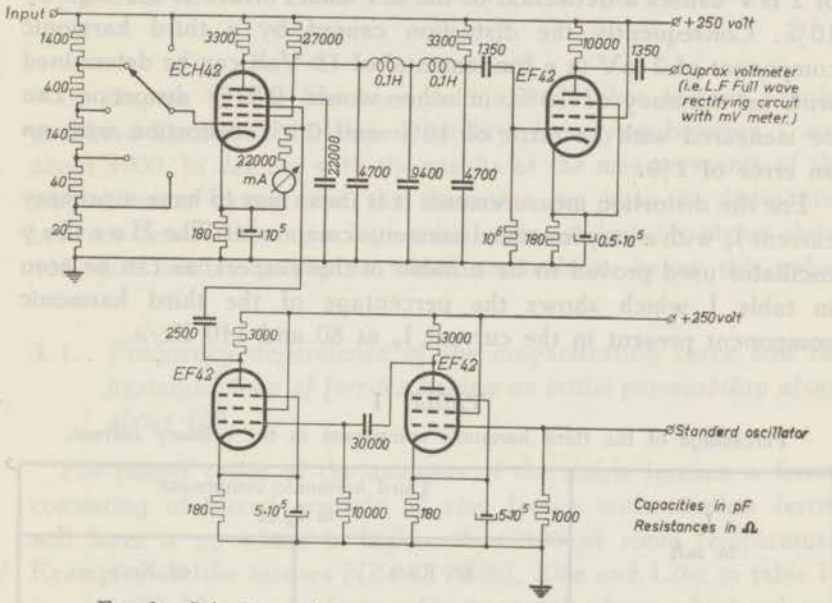

Fig. 9. Selective voltmeter used for distortion measurements. (For ECH 42 read ECH 21).

The input resistance of the selective voltmeter is 2000 Ohm. This value is chosen on the one hand to have a low secondary transformer current **) and on the other to ascertain that the attenuator is frequency independent up to at least 4.5 Mc/s (the third harmonic of the highest measuring frequency). The cut-off frequency of the low-pass filter is 8 Kc/s and at 25 Kc/s the attenuation factor of this filter is one thousandth. The maximum sensitivity of the instrument is determined by both the maximum voltage which can be supplied by the low-frequency amplifier without any change in its amplification factor (*i.e.* 18 Volt), and by the output voltage of the amplifier in the case of a short-

*) Philips GM 4132 cuprox voltmeter. A low-frequency amplifier with full-wave rectifier.

**) For these measurements the number of the secondary turns is always very small, e.g. 1 or 2 so that the conditions [7] are always fulfilled for the secondary.

circuited input. The latter voltage is limited to 1 mV by a suitable earthing circuit and by feeding the cathodes of the amplifier with direct current. What is left consists of noise and 50 c/s hum and is not additive to the measuring voltage, for a known voltage of 2 mV causes a deflection of the mV-meter which is too high by 10%. Consequently the distortion caused by a third harmonic component of 2 mV in a fundamental of 18 Volt can be determined with an accuracy of 10%, in other words 0.01% distortion can be measured with an error of 10% and 0.1% distortion with an an error of 1%.

For the distortion measurements it is important to have a primary current I_p with a very low third harmonic component. The Hartley oscillator used proved to be suitable in this respect, as can be seen in table I which shows the percentage of the third harmonic component present in the current I_p at 80 and 140 Kc/s.

TABLE I

Percentage of the third harmonic component in the primary current.

I_P in mA	Third harmonic component in I_p at	
	80 Kc/s	140 Kc/s
16	0.05 %	0.03 %
21	0.05 %	0.05 %
31	0.16 %	0.08 %
42	0.20 %	0.20 %

3. RESULTS OF THE MEASUREMENTS OF MAGNETIZATION CURVES AND DISTORTION

In chapter 1. 1. it has been said already that ferrites can be produced having an initial permeability μ_o varying between 1 and about 4000. In dealing with the results of the measurements of the magnetization curves and the distortion we wish to distinguish between ferrites having a high initial permeability, *i.e.* above about 400, and ferrites having an initial permeability below this value.

3. 1. *Frequency dependence of the magnetization curve and the hysteresis loop of ferrites having an initial permeability above about 400.*

For proper ratios of the amounts of the single ferrites, a ferrite consisting of mixed crystals of zinc ferrite with another ferrite will have a μ_o which is higher than 400 at room temperature. Examples are the ferrites NZ4A, 1098d, 708e and L26c in table II, see page 33. Manganese ferrous ferrite can also have a high value of the initial permeability *), *e.g.* ferrite 640e in table II for which $\mu_o = 860$. For these ferrites the magnetization curves have been measured as a function of frequency up to 600 Kc/s. The results of these measurements for ferrite 640e are shown in figure 10. The low-frequency magnetization curve (0.5 Kc/s) has the well-known shape: at sufficiently low field strengths B_{max} is proportional to H_{max}, hence $B_{max} \approx \mu_o H_{max}$ and at higher field strengths the amplitude permeability μ, ($B_{max} = \mu H_{max}$), increases with increasing H_{max}, reaching a maximum value for $H_{max} = 0.6$ Oersted and decreasing then monotonically to the value 1 for very high field strengths. The shape of the magnetization curve of this ferrite depends on the frequency of the field, and for high frequencies it becomes a straight line, its slope being the same as the initial slope

*) This is brought about by the fact that in manganese ferrous ferrite the magnetostriction at room temperature is very small, which might be caused (13) by a cancelling of the negative magnetostriction of $MnFe_2O_4$ and the positive magnetostriction of Fe_3O_4.

of the low-frequency magnetization curve, μ_o. Thus the above defined amplitude permeability μ for a definite H_{max} depends on frequency. This is illustrated in the inset of figure 10, which shows this change with frequency for the permeability at 0.6 Oersted. An obvious interpretation of this behaviour is that there are two independent magnetization processes. One process which gives rise to μ_o, is frequency independent up to 626 Kc/s (μ_o drops to half of its low frequency value only at 5 Mc/s, see table II and chapter 7. 2), and a second process gives an important contribution to the magnetization at field strengths of about the coercive force H_c. This second process is already very frequency dependent from 100 Kc/s onwards.

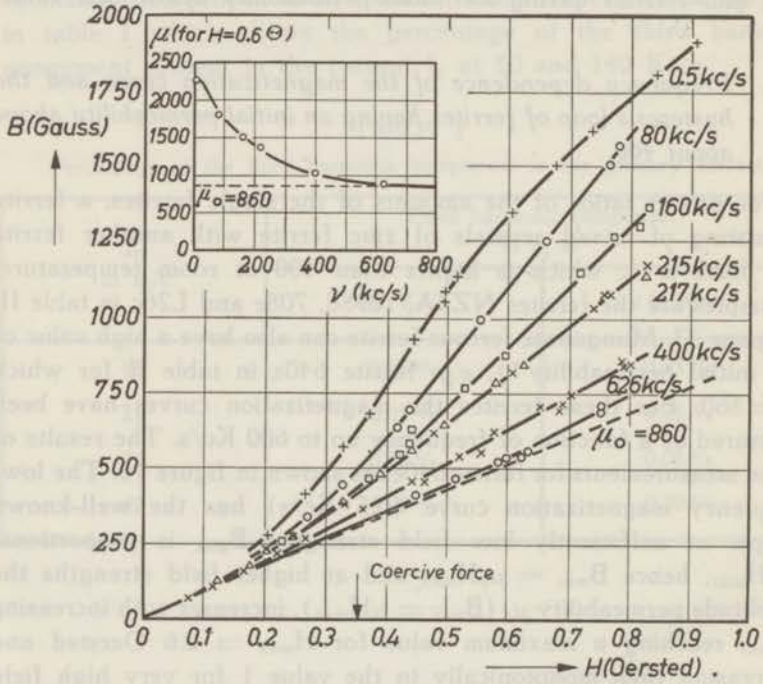

Fig. 10. Frequency-dependent magnetization curves of ferrite 640e. Inset: μ as a function of frequency for H = 0.6 Oersted.

The magnetization curves of the ferrites NZ4A, 1098d, 708e and L26c of table II (all of them having $\mu_o > 400$) show the same behaviour as a function of frequency as is found for ferrite 640e in figure 10. The only difference is that at 600 Kc/s these curves for the ferrites NZ4A and L26c are still not a straight line.

Distortion measurements for ferrites, as described in chapter 2. 3, can give information on the loop that gives the relation between the field strength and the induction in the core during one period of the sinusoidal field H (quasi-statically measured, it is the hysteresis loop). It is to be expected that this loop will also depend on frequency when the magnetization curve does. Figure 11 gives

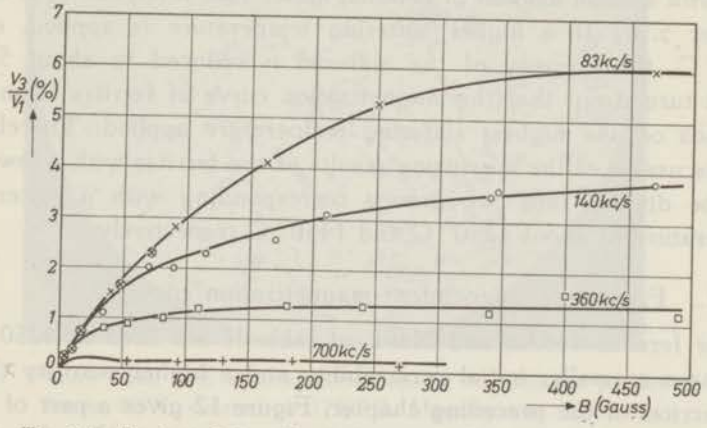

Fig. 11. Ferrite 640e. Distortion *versus* induction at several frequencies. ⊗ Distortion at 2 Kc/s calculated from the hysteresis resistance according to formula [15].

for the ferrite 640e the results of the distortion measurements at four frequencies. It is seen that this quantity depends very much on frequency, being almost absent at 700 Kc/s. Thus for this ferrite the shape of the hysteresis loop must likewise change with frequency: at low frequency it is the well-known loop with sharp tips, whereas at high frequency B is a linear function of H and only a phase shift between the two can occur (see chapter 8. 3), giving rise to an elliptical loop. For all ferrites investigated, the frequency dependence of the magnetization curve and the distortion go hand-in-hand.

3. 2. *Frequency dependence of the magnetization curve and the hysteresis loop of ferrites having an initial permeability below about 400.*

The ferrites described in the preceding chapter, *i.e.* the manganese ferrites and the mixed ferrites with a high zinc content, have a high initial permeability and a small porosity.

In chapter 1. 1. it has already been said that a reduction of the zinc content always results in a decrease of permeability. However, a decrease of the zinc content is at constant sintering temperature always attended by an increase of the porosity. The usual sintering temperature is 1250° C and porosities of 25% can occur. This rather low sintering temperature is important for producing ferrites with a small amount of residual losses (see reference (13) and chapter 5. 3.) If a higher sintering temperature is applied, *e.g.* 1450° C, the porosity of the material is reduced to about 5%, and it turned out that the magnetization curve of ferrites strongly depends on the highest sintering temperature applied. Therefore the discussion of the measuring results of the ferrites with a low μ_0 will be divided into two groups corresponding with a sintering temperature of about 1250° C and 1450° C respectively.

3. 2. 1. Frequency-independent magnetization curve.

The ferrites 448Aa and N89L of table II are fired at 1250° C and have a smaller initial permeability and a higher porosity than the ferrites of the preceding chapter. Figure 12 gives a part of the magnetization curves of the nickel zinc ferrite 448Aa for five different frequencies. An obvious difference with similar curves for the ferrites with a high μ_0 is the large field strength at which μ has its maximum value. In figure 12 this field strength is still not

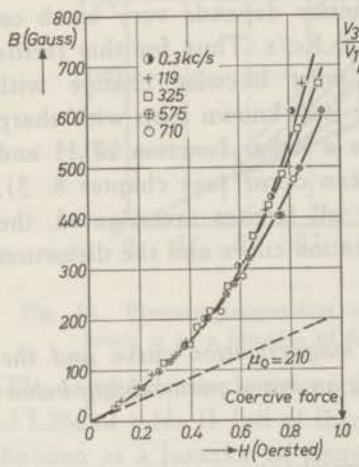

Fig. 12. Ferrite 448Aa. Nearly frequency-independent magnetization curve.

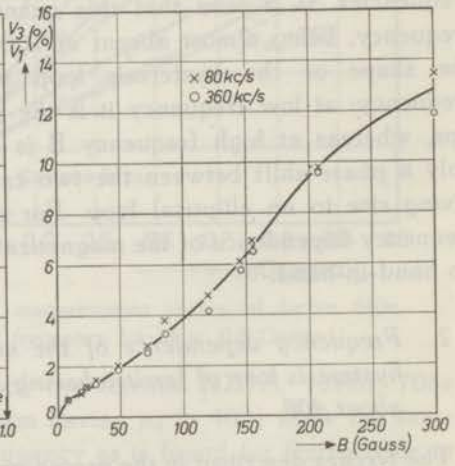

Fig. 13. Ferrite 448Aa. Nearly frequency-independent distortion.

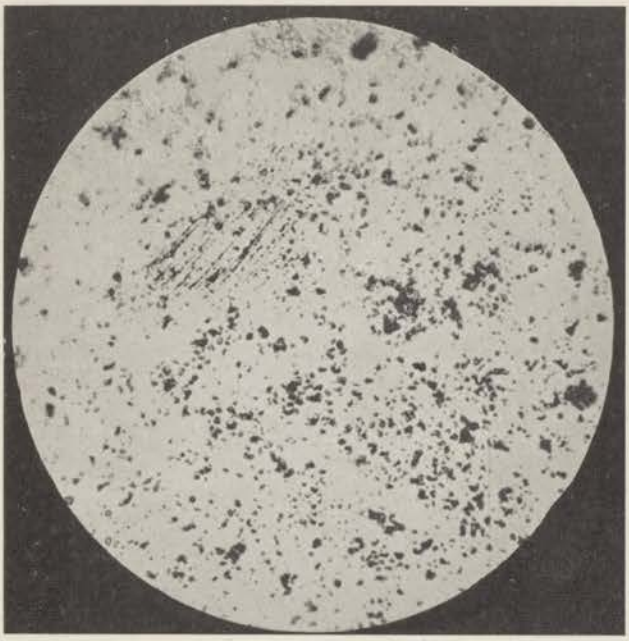

Fig. 14. Picture taken with a metal microscope of the polished surface of the ferrite N89L sintered at 1250° C. Magnification 500×.

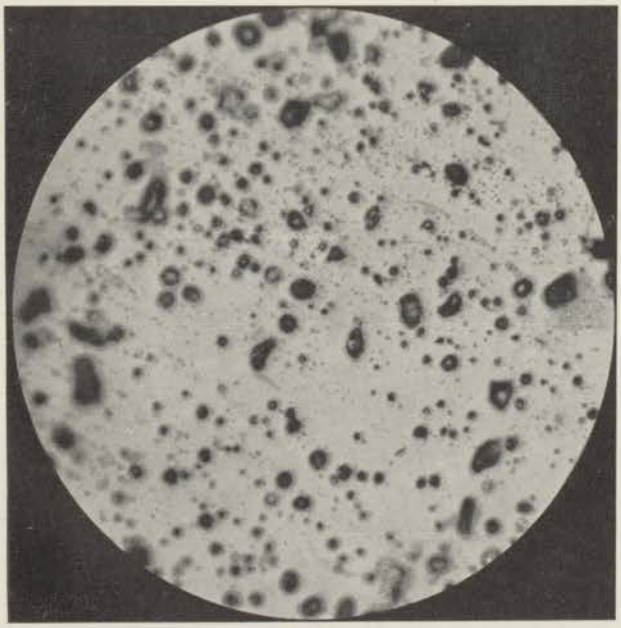

Fig. 15. Do. for ferrite 834Ae which has been sintered at 1450° C.

reached because of the limited oscillator current and the limitations imposed on the number of turns by the conditions [6] and [7]. However, it can yet be seen that in this case the magnetization curves are almost frequency-independent. For ferrites having a still smaller initial permeability, these curves appeared to be invariable up to at least 1 Mc/s.

When the magnetization curve does not depend on frequency, we must also expect a frequency-independent hysteresis loop, and consequently a frequency-independent distortion. This is actually found for ferrite 448Aa, as can be seen in figure 13. Similar results have been obtained for the nickel zinc ferrite N89L (see the next chapter and the figures 16 and 20).

3. 2. 2. Frequency-dependent magnetization curve.

Ferrite 834Ae (see table II) has the chemical composition in mol % 27 NiO, 23 ZnO and 50 Fe_2O_3, and is fired at 1450° C in oxygen. We shall compare the properties of this ferrite with those of a ferrite having approximately the same chemical composition, but which is fired at a lower temperature, for instance ferrite N89L of table II (chemical composition in mol % 25 NiO, 25 ZnO and 50 Fe_2O_3) which is fired at 1250° C. The figures 14 and 15 are photographs taken with a metal microscope of polished surfaces of these ferrites. The magnification is 500 ×. The white areas are the surfaces of the ferrite and the black areas are holes. It is likely that the surface holes are enlarged by the polishing process so that a picture of the micrograph shows too high a porosity. Nevertheless it becomes clear from the pictures that after sintering at 1450° C the number of holes is diminished and their average size enlarged. No second phase could be detected with the metal microscope, though ferrite 834Ae contains 0.8 per cent by weight of ferrous ions.

The high firing temperature has little effect on the initial permeability which is 218 for the porous and 312 for the non-porous material. (This difference can partly be accounted for by the unequal densities of the ferrites, which are 4.55 and 5.21 respectively, so that the increase of μ_0 after sintering at 1450° C is about 25%). A much greater difference, at least at low frequency, is found between the magnetizations at a higher field strength. For instance at a field strength of 0.75 Oersted the inductions in the ferrites fired at 1250° C and 1450° C are 205 and 1470 Gauss

respectively; the additional firing results in an increase of the induction by a factor of 7 (cf. the figures 16 and 17).

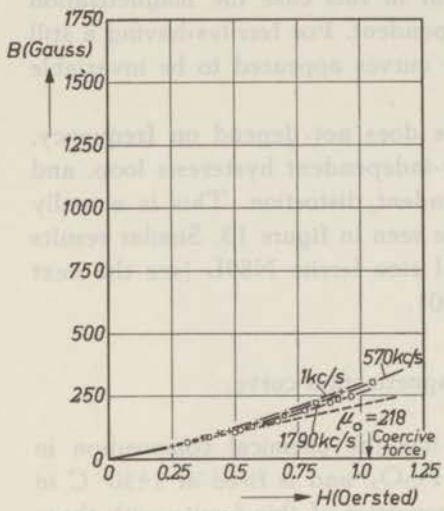

Fig. 16. Magnetization curves of ferrite N89L (fired at 1250° C).

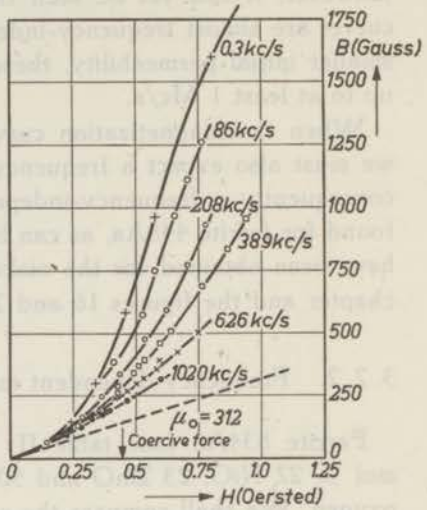

Fig. 17. Do. for ferrite 834Ae (of about the same chemical composition as N89L but fired at 1450° C).

The curves for the ferrite 834Ae, which is sintered at a high temperature, depend much on frequency, as is also shown in figure 17. It can be seen that the additional magnetization process which makes a large contribution to the magnetization in this dense ferrite, is strongly dependent on the frequency and it makes only a small contribution at 1020 Kc/s. On the contrary the initial permeability in both cases remains constant up to 10 Mc/s. This is the same phenomenon as is already found for ferrites with a high value of μ_o, and which is discussed in chapter 3. 1.

The frequency dependence of the magnetization curves of the ferrite which is sintered at 1450° C is again well demonstrated in the results of the distortion measurements. The three curves in figure 18 give the relation between the distortion and the amplitude of the induction at 80, 360 and 590 Kc/s respectively. These curves are similar to those for a ferrite having an initial permeability above about 400, but for one exception, *i.e.* that, apart from the frequency-dependent distortion, at low inductions a frequency-independent distortion arises. At 590 Kc/s the distortion curve is easily divided into two parts given by the curves OA and ODE.

Subtracting the distortion given by the curve ODE from the measured curves at 80 and 360 Kc/s we get the dotted lines OA′ and OA″ in figure 18 which are quite similar to the distortion curves for the ferrite 640e in figure 11. It is to be concluded that the distortion caused by ferrites sintered at 1450° C is brought about by two magnetization processes, one process which is

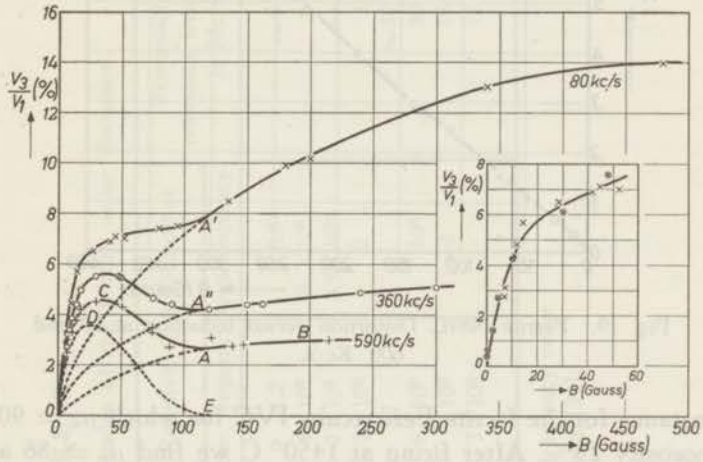

Fig. 18. Ferrite 834Ae. Distortion *versus* induction for several frequencies. Inset: × Distortion measurements at 80 Kc/s with selective voltmeter. ⊗ Distortion at 2 Kc/s calculated from the hysteresis resistance according to formula [15].

frequency dependent and is found for all ferrites of chapter 3. 1, and another process which is, in the frequency range covered, independent of the frequency. These peculiar distortion curves are not found for the normally fired ferrite N89L, for which the curves are represented in figure 19.

As will be described in chapter 4. 4, the distortion caused by an irreversible process can be calculated from the hysteresis losses. At 2 Kc/s the hysteresis resistance of ferrite 834Ae has been measured at small field strengths and afterwards the distortion was calculated. The results are given in the inset of figure 18, in which the encircled crosses indicate the distortion which is calculated from the hysteresis resistance at 2 Kc/s, and the crosses represent the distortion as it is measured with a selective voltmeter at 80 Kc/s (in the large figure the latter are also given on a smaller scale). The good agreement between both warrants the conclusion that at 80 Kc/s and at small field strengths the distortion is caused by an irreversible magnetization process. Consequently the frequency-independent part of the distortion is also caused by an irreversible process.

When ferrites which have an initial permeability that is substantially smaller than 200 are fired at 1450° C, the magnetization curve does not depend on frequency up to 1.5 Mc/s. This is found

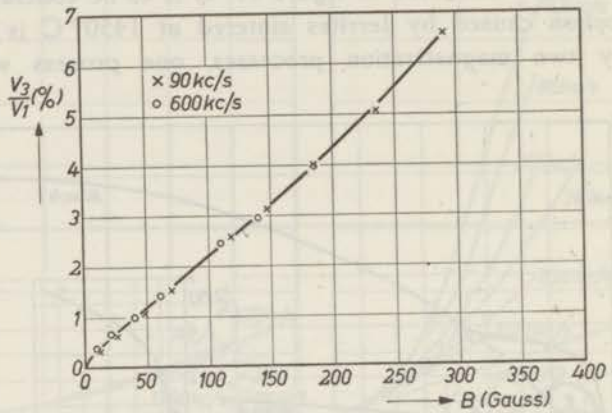

Fig. 19. Ferrite N89L. Distortion *versus* induction at 90 and 600 Kc/s.

for instance for the ferrite Ferroxcube IVC for which $\mu_o = 90$ and the porosity 23%. After firing at 1450° C we find $\mu_o = 86$ and a porosity of 8% (see table III). The induction at a field strength of 1.2 Oersted has increased from 150 to 1400 Gauss, similarly to what was found for ferrite 834Ae, and at 1100 Kc/s the same magnetization curve is found as at lower frequencies. Summarizing, we can say that a frequency-dependent magnetization curve is always found for the ferrites having an initial permeability above 400. For ferrites having a smaller initial permeability and having been fired at a relatively low temperature (about 1250° C) the magnetization curve remains unaltered up to at least 1.5 Mc/s. The broad limit marked by the value of μ_o is shifted to lower μ_o-values when the ferrite is fired at a higher temperature.

TABLE II

Chemical composition and characteristics of the ferrites under discussion.

Ferrite	Composition in mol % (balance Fe_2O_3 + FeO)				μ_0	Porosity in %	Resistivity ϱ in Ohmcm at		Ferromagnetic resonance frequency*) in Mc/s	$\frac{1}{\tau}$ **) in Kc/s
	NiO	MnO	ZnO	Li_2O			low frequency	high frequency		
640e		43.5			860	~5	1.2	0.6	~5	83
NZ4A	18.5		32		945	~8	4×10^6	8×10^5	6	280
1098d		30	22.5		740	~6	2×10^5	8.5×10^3	—	175
708e		23	25		1300	~5	2×10^2	2	3	140
448Aa	25		20		210	~10	52		~30	>2000
N89L	25		25		218	14.6	6×10^6	10^5	30	>2000
834Ae	27		23		312	3.2	10^3	~2	16	115
L26c			33	9	430	4.6	2×10^2		12	~ 300

*) The frequency at which μ' has decreased to half of its low frequency value.

**) The quantity τ is the time constant in the relaxation formula [34].

4. THE ADDITIONAL MAGNETIZATION PROCESS IN FERRITES AT FIELD STRENGTHS OF THE ORDER OF MAGNITUDE OF THE COERCIVE FORCE

4. 1. *Introduction.*

In general in a demagnetized state a polycrystalline ferromagnetic material will consist of homogeneously magnetized Weiss domains which are separated by regions in which the direction of the electron spins changes gradually from the preferential direction in one Weiss domain to that of the neighbouring domain. This region is called a domain wall (18, 19). Bitter (20) was the first who could confirm this experimentally. He made the domain structure visible under a microscope by bringing colloidal Fe_2O_3 upon a polished surface of a ferromagnetic alloy. Recently improved experiments have been carried out with great success by Williams, Bozorth and Shockley (21) with single crystals of silicon iron.

The magnetization of a ferromagnetic material by an externally applied field can take place by two processes:

i. *a rotation process.* The joint magnetic spins in a Weiss domain turn from their preferential direction in the material so as to approach the direction of the external field.

ii. *a domain-wall displacement.* The walls between two Weiss domains will move so that those domains that have the more favourable spin orientation with respect to the field, grow at the expense of the others.

The rotation processes and the wall displacements can both be divided into a reversible and an irreversible type, depending on whether the original magnetic state is restored or not after the magnetic field is switched off. A detailed discussion of these processes is given by Bozorth (22). Still little is known about the ways in which the magnetization in ferrites is caused. As these materials are very porous it can be expected that the processes occur in another sequence in relation to the magnetization curve than what is known to be the case for metals.

From the results of the measurements given in chapter 3 it is

clear that in ferrites different magnetization processes occur. In this chapter we will discuss particularly the additional process which is found to play a part at field strengths of the order of magnitude of the coercive force, at least at low frequencies in ferrites having a high initial permeability. This process also causes the non-linearity of ferrites at low frequency, as can be concluded from the measurements of the distortion (fig. 11). The following experiments have been carried out to get an indication of the nature of this magnetization process:

i. the field strength at which these processes give a great contribution to the magnetization has been determined for ferrites with various porosities.

ii. the influence of externally applied stresses upon the contribution of this magnetization process has been examined. We have applied a homogeneous stress such that the electron spins are forced either into a direction parallel or into a direction perpendicular to the external magnetic field.

4.2. *The influence of the porosity on the magnetization curve of ferrites.*

The ferrites that have been investigated by us, are polycrystalline sintered oxides. The porosity of these ceramics depends on their sintering temperature. The pores in the final product will determine its magnetic properties to a large extent. The influence of the pores upon the coercive force of a ferromagnetic material has first been studied by Kersten (23) and later by Néel (24) in his article "Bases d'une nouvelle théorie générale du champ coercitif". It follows from both theories that in a ferromagnetic material the domain walls will extend preferentially from pore to pore. According to Kersten the walls are fixed on the pores, thus by minimizing their area also minimizing the total wall energy, which is proportional to it. Néel points to the fact that the internal stray fields, which always are generated by the inclusions in a ferromagnetic material, will be confined to small regions around the inclusions when they are situated on the boundaries between Weiss domains. An external magnetic field can exercise a force upon a domain wall. The direction of this force is such that the adjacent Weiss domain grows in which the magnetization makes the smaller angle with the external field. The magnitude of the moving force is proportional to the area of the wall. If it is assumed that in ferrites

the domain walls extend from pore to pore then the smallest field strength to detach the walls from the pores will be required for those ferrites in which the porosity is caused by few pores having a diameter comparable with the thickness of the wall. In ferrites of the same chemical composition the irreversible domain-wall displacements will take place at a lower field strength when the ferrite is less porous or when its porosity is formed by few large pores. This has been verified for instance for the ferrites N89L and 834Ae of table II, which have been fired at 1250° C and 1450° C respectively. (See the figures 14 and 15). The porosities obtained are 14.6% and 3.2% and the coercive forces correspondingly 1.03 and 0.42 Oersted (though μ_0 has not changed very much). From a comparison of the low-frequency magnetization curves of these ferrites, as given in the figures 16 and 17, also follows that a high temperature firing gives a large increase of the contribution of the additional magnetization process at relatively small values of the external field. This also suggests that this process is related to domain-wall displacements.

TABLE III

Relation between porosity and coercive force of nickel zinc ferrites.

Ferroxcube IV		Chemical composition in mol % (balance $FeO + Fe_2O_3$)		Porosity p in %	Saturation magnetization I_s in Gauss	Initial permeability μ_0	Coercive force in Oersted	
Grade	Firing temperature in °C	NiO	ZnO				according to formula [9]	measured
A	1250	17.5	33.2	8.9	292	650	0.5	0.4
B	1250	24.9	24.9	15.4	332	230	2.5	1.4
C	1250	31.7	16.5	22.5	321	90	7.7	4.0
D	1250	39.0	9.4	24.3	283	45	12.8	6.8
E	1250	48.2	0.7	24.8	196	17	19	13.7
A	1450	see above		9.5	290	470	0.7	0.3
B	1450			3.2	380	312	0.4	0.4
C	1450			8.0	381	86	3.3	1.1
D	1450			8.9	341	63	4.2	1.7
E	1450			9.9	235	42	4.5	3.2

It is of interest to examine the correlation between the coercive force H_c and the porosity p for nickel zinc ferrites with widely differing properties. The

porosity p is defined as the proportion of pores in the ferrite that can be infered from a comparison of the apparent density with the X-ray density. The latter is deduced from the lattice constants as given by Guillaud (25). Table III gives the measuring results for p and H_c for samples of different chemical composition, which have been fired at 1250° C and 1450° C. It can be infered that in general a low porosity goes hand-in-hand with a low coercive force. Starting from the assumption that the coercive force depends on irreversible domain-wall displacements, Kersten (23) and Néel (24) derived a relation between H_c and p. The first order crystal anisotropy constant K_1 (K_2 has been neglected) and the saturation magnetization I_s occur in the equations of these authors. For ferrites K_1 is not known. However the value of K_1 can be derived from the measured value of the initial permeability μ_0 if it is assumed that for ferrites μ_0 is mainly determined by rotations (this will be discussed in chapter 7.2). It appears that Kersten's equation leads to a value for H_c which is too small by a factor of 10. (This factor is still increased when Néel's extension of Kersten's theory for an arbitrary distribution of the inclusions is taken into account). According to the new theory of Néel, the coercive force of ferromagnetic materials with negative crystal anisotropy, as the ferrites are (see chapter 7. 2), is in the case of arbitrary distributed inclusions given by the formula

$$H_c = \frac{4K_1 \cdot p}{3\pi I_s} \cdot \left[0.39 + \tfrac{1}{2} \ln \frac{3\pi I_s^2}{K_1} \right] . \qquad [9]$$

In the case of pure rotation processes K_1 is related to μ_0 by the formula

$$\mu_0 - 1 = \frac{8\pi}{3} \cdot \frac{I_s^2}{K_1} . \qquad [10]$$

In the last but one column of table III the results are given for the coercive force as calculated according to the formulae [9] and [10]. The calculated values of H_c are greater than the measured values. This is plausible since only those pores contribute to the coercive force that have a diameter comparable with the thickness of the domain walls in the ferrite. In view of the simplifications made, there is a good agreement between the calculated and the measured values of H_c and it can be concluded that in ferrites the pores determine the coercive force to a large extent.

4. 3. *The influence of external stresses on the magnetization curve of ferrites.*

A further confirmation of our ideas concerning two different magnetization processes will be obtained if we succeed in measuring the magnetization curve of the same ferrite under such conditions that one of these processes is inhibited. This is realized for ferrites under an external stress. The mixed nickel zinc ferrites have a negative saturation magnetostriction constant λ_s. If a tensile stress is applied to a rod of this kind of ferrites, the magnetic spins will turn from their preferential direction in the internal anisotropy fields into a direction perpendicular to the direction of this stress.

For large stresses the situation is obtained that all spins are directed perpendicularly to the axis of the rod. Consequently an external field parallel to the axis of the rod exerts no force on the domain walls and the magnetization of the rod into the direction of its axis can be brought about merely by a joint reversible rotation of the spins in each Weiss domain. Domain-wall displacements cannot give a contribution to the magnetization. Inversely an axial pressure upon the rod will cause the spins to be oriented parallel to the axis of the rod so that the domain walls are parallel to this axis too. In this case 180°-wall displacements will contribute very much to the magnetization in an axial field, whereas rotation processes are excluded. In figure 20 commutation curves are given which have

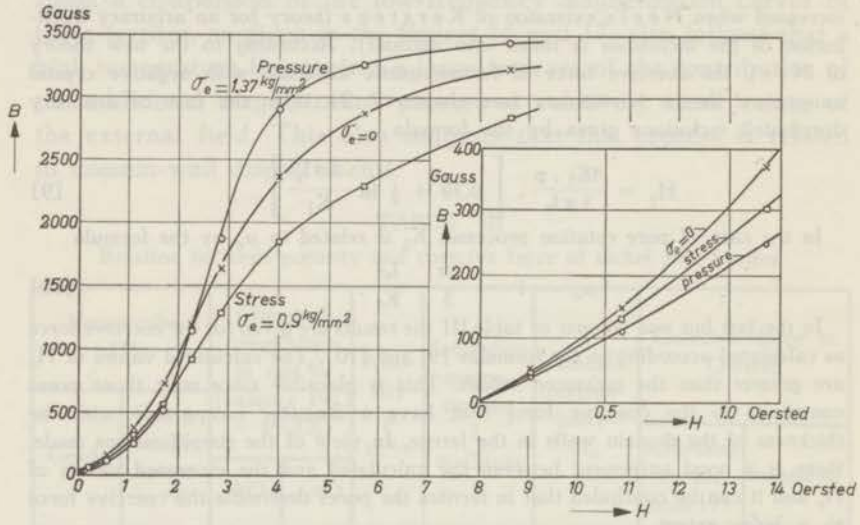

Fig. 20. Commutation curve for a rod of "Ferroxcube IV*B*" under different stresses.

been measured by Mr J. F. Fast on rods of "Ferroxcube IV*B*" under externally applied stress and pressure. (For the chemical composition see table III). For comparison, the curve taken without external stress is inserted in the same figure. Though the applied stresses are not sufficient to accomplish a complete spin orientation (because of the low tensile strength of the ferrite), a marked influence upon the magnetization curve is found. The applied external stress and pressure both decrease the permeability for small magnetic fields, but from about 2 Oersted,

i.e. where the additional magnetization process comes into play, stress and pressure have an opposite influence. The external tensile stress of 0.9 kg/mm² decreases the permeability whereas it is increased by a pressure of 1.37 kg/mm².

From these experiments it can be concluded that the additional magnetization process which comes into play at field strengths of about the coercive force, is related to displacements of the boundaries between W e i s s domains.

4. 4. *Losses caused by irreversible magnetization processes.*

The distortion caused in a network by a coil with a ferromagnetic core is due to the non-linear relation existing between the induction B and the field strength H in the core. This non-linearity can have two reasons:

a. *B is a non-linear function of H, but it is a single-valued function of H.* After demagnetization of the core, the function B(H) will have the origin (H = 0, B = 0) as a point of symmetry, thus B(H) = —B (—H). For small values of H the function B(H) can be developed into the series

$$B(H) = \mu H + \nu H^3 + \lambda H^5 + \ldots . \qquad [11]$$

from which it follows that for a field $H = H_{max} \cos \omega t$ the distortion $D = \frac{V_3}{V_1}$ is proportional to H^2_{max}.

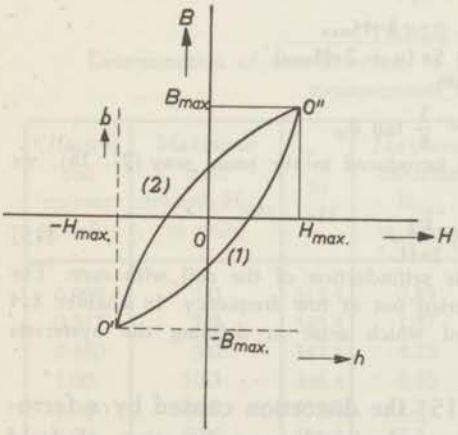

Fig. 21. The hysteresis loop at low inductions.

b. *B is a bivalent function of H.* This means hysteresis. Also in this case the origin has to be a point of symmetry. The most simple representation for the lower branch (1) of the hysteresis loop is given by

$$b(h) = \mu h + \nu h^2, \qquad [12]$$

if the co-ordinates b and h have te lower tip O′ of the loop as the origin, see figure 21. The upper branch (2) is given by an analogous equation with respect to co-ordinates having O″ as the origin.

After a simple transformation to co-ordinates B and H with O as the origin, both branches are given by the formula

$$B(H) = \mp \nu H^2_{max} + (\mu + 2\nu H_{max})\, H \pm \nu H^2 . \qquad [13]$$

For a sinusoidal field $H = H_{max} \cos \omega t$ it can be seen that in this case the distortion $D = \frac{V_3}{V_1}$ is proportional to H_{max}. So for sufficiently small fields the distortion will entirely be caused by hysteresis, as Peterson (26) has shown already after a detailed calculation.

From equation [13] a simple relation can be derived between the distortion and the hysteresis resistance in ferromagnetic materials. The equation can be written as

$$B(t) = (\mu + 2\nu H_{max})\, H_{max} \cos\omega t \mp \nu H^2_{max} \sin^2 \omega t ,$$

or after a series development of the last term,

$$B(t) = (\mu + 2\nu H_{max})\, H_{max} \cos\omega t - \frac{8\nu}{\pi} H^2_{max} \left(\frac{1}{3} \sin\omega t - \frac{1}{3 \cdot 5} \sin 3\omega t + \cdots\right).$$

The coil voltage E is

$$E/c = -\frac{dB(t)}{dt} = -(\mu + 2\,\nu H_{max})\, \omega\, H_{max} \sin \omega t + \frac{8\nu}{\pi}\, \omega\, H^2_{max} \left(\frac{1}{3} \cos \omega t - \frac{1}{5} \cos 3\omega t\right),$$

where c depends on coil dimensions and core constants. The loss factor $\tan \delta$ for the coil is defined as

$$\tan \delta_H = \frac{8\,\nu H_{max}}{3\pi\,(\mu + 2\,\nu H_{max})}. \qquad [14]$$

and the distortion D is defined as

$$D = \frac{V_3}{V_1} = \frac{8\,\nu H_{max}}{5\pi\,(\mu + 2\,\nu H_{max})}.$$

Consequently there exists the relation

$$D = \frac{3}{5} \tan \delta_H .$$

If the hysteresis resistance R_h is introduced in the usual way (27, 28), we find the well-known relation

$$D = 0.6\, \frac{R_h}{2\pi f L}, \qquad [15]$$

where f is the frequency and L the selfinduction of the coil with core. The testing of this relation must be carried out at low frequency. In chapter 8.4 the complications will be discussed which arise in defining the hysteresis resistance at higher frequencies.

With the help of formula [15] the distortion caused by a ferromagnetic core material can be calculated as a function of field strength, when the loss resistance of a coil with such a core is measured in dependence of the coil current. This has actually

already been done for ferrite 834Ae, as described in the small print of page 31. The results are given in figure 18. In the following a more detailed description of the measuring procedure will be given. The measurement can easily be carried out in a Maxwell-bridge circuit as given in figure 22. The branches of the bridge consist of

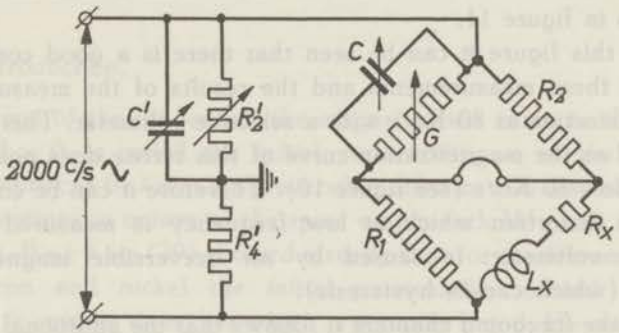

Fig. 22. Maxwell-bridge circuit for measuring the complex impedance of a coil.

two normal resistances R_1 and R_2, the unknown self inductance L_x with loss resistance R_x, and in the fourth branch a variable condenser C with a variable conductivity G in parallel. To avoid difficulties with self capacities, the bridge is equipped with a Wagner earth. The bridge itself was constructed by Dr. J. W. Köhler and Ir. C. G. Koops † of this laboratory.

TABLE IV

Determination of the distortion of ferrite 640e from the hysteresis measurements at 2 Kc/s.

Effective coil current in mA	Maximum field strength H_{max} in mOe	L_x in μH	Maximum induction B_{max} in Gauss	R_x in Ω	R_h in Ω	$D = \frac{V_3}{V_1}$ in %, calculated according to formula [15]
0.099	1.0	341.4	0.85	0.322	0.001	0.01[4]
0.217	2.2	342.4	1.87	0.326	0.005	0.07
0.480	5.0	343.1	4.25	0.334	0.013	0.18
1.00	10.3	346.4	8.85	0.345	0.024	0.33
1.96	20.2	353.0	17.7	0.371	0.050	0.68
4.90	50.6	376.7	47.3	0.448	0.127	1.61
7.0	72.3	393.2	70.5	0.509	0.188	2.28
0.100	1.0	337.3	0.84	0.320		

Table IV gives the results of the measurements of the hysteresis resistance of a coil consisting of a toroidal core of ferrite 640e provided with 46 turns. The dimensions of the core are: internal and external diameter 2.10 and 2.94 cm respectively and a cross section of 0.42×0.29 cm^2. From the measuring results the distortion is calculated, this is shown in the last column of the same table, and also in figure 11.

From this figure it can be seen that there is a good conformity between these measurements and the results of the measurements of the distortion at 80 Kc/s with a selective voltmeter. This is to be expected as the magnetization curve of this ferrite does not change much below 80 Kc/s (see figure 10). Therefore it can be concluded that the distortion which at low frequency is measured with a selective voltmeter, is caused by an irreversible magnetization process (which causes hysteresis).

From the foregoing chapters it follows that the additional magnetization process which gives rise to the non-linear behaviour of the ferrites consists of irreversible displacements of domain walls.

5. PROPERTIES OF THE MAGNETIZATION PROCESS IN FERRITES AT VERY SMALL FIELD STRENGTHS

5. 1. *Introduction.*

The slope of the tangent of the magnetization curve in the point $H = 0$, $B = 0$, is called the initial permeability μ_0 of the ferrite. This quantity can be a result of reversible domain-wall displacements and of rotations in unison of the spins within each Weiss domain, or of both. Becker (29) showed already that for the ferromagnetic metals iron and nickel the initial permeability caused by the rotations is smaller than that which is actually found. He concluded therefore that for these metals the high value of μ_0 is related to reversible domain-wall displacements. For alloys it is still an open question which magnetization process takes place at very small field strengths. Bozorth (30) suggests that for the nickel iron alloys having a high permeability, the rotations in unison might give the predominant contribution to the initial permeability. In the case of ferrites some indirect experiments can give information on this problem, and in this chapter the frequency *spectrum* of the initial permeability of the ferrites will therefore be studied.

As the losses generated in a magnetic core when it is subjected to an alternating magnetic field will play an important role, we shall discuss briefly a formal representation of these losses and a way of separating these losses into different types.

As is known a coil with core in which losses are generated can be treated as a self inductance in series with a resistance. Consequently the permeability of the core material may be regarded as a complex quantity, and it can be written:

$$\mu = \mu' - j\,\mu'', \qquad [16]$$

when the influence of higher harmonics can be neglected, which is mostly the case at small field strengths. The phase angle δ between the induction and the sinusoidally varying magnetic field in the ferrite is defined by the relation

$$\tan \delta = \frac{\mu''}{\mu'} \quad . \qquad [17]$$

The possibility of separating the losses in ferromagnetic materials into three types has already been discussed many times (27, 28, 31). These three types of losses are the following.

i. *Hysteresis losses*, which are discussed for ferrites in the chapters 4. 4. and 8.

ii. *Eddy-current losses*, which can be caused by both macro and micro eddy-currents. The former are induced through the whole core as a consequence of the change of induction in the material. The latter are localized round a moving domain wall or rotating spins, and Williams, Shockley and Kittel (32) have estimated that for a special configuration these micro eddy-current losses are even higher than the macro eddy-current losses. These kinds of losses are negligibly small for the ferrites with a high resistivity.

iii. *Residual losses*. When for ferrites, even in the case of negligibly small eddy-current losses, the loss factor $\tan\delta$ is plotted against the maximum induction B_{max}, a straight line is obtained showing after extrapolating to zero induction a residual loss factor $\tan\delta_r$. At room temperature $\tan\delta_r$ has a fairly constant value at low frequencies, but at higher frequencies the loss factor rises to high values, which will be seen in chapter 5. 2. In chapter 5. 3 we shall deal with some experiments concerning the rather constant level of the loss factor $\tan\delta_r$ at low frequency.

5. 2. *The kind of the magnetization process in ferrites at very small field strengths.*

5. 2. 1. Frequency spectrum of the initial permeability of ferrites at room temperature.

For a number of ferrites with widely varying values of the initial permeability the real and imaginary part of μ_o have been measured as a function of frequency by Dr. M. Gevers and Mr. C. M. van der Burgt (see Snoek and Beljers (33)), using the coaxial line resonance method (16). In figure 23 the results of similar measurements are given which, in co-operation with Mr. C. M. van der Burgt, have been carried out for samples of nickel zinc ferrite with various nickel zinc ratios. Their chemical compositions are given in table III. The real part of the initial permeability, μ', has a constant value at low frequencies, but after a very small increase, it decreases to low values at high frequencies. The

imaginary part μ'' has a pronounced maximum just at the frequency where μ' drops most strongly. For the various ferrites this dispersion frequency is closely related to the value of μ_o at low frequency, and it can be seen that the product of both is approximately a

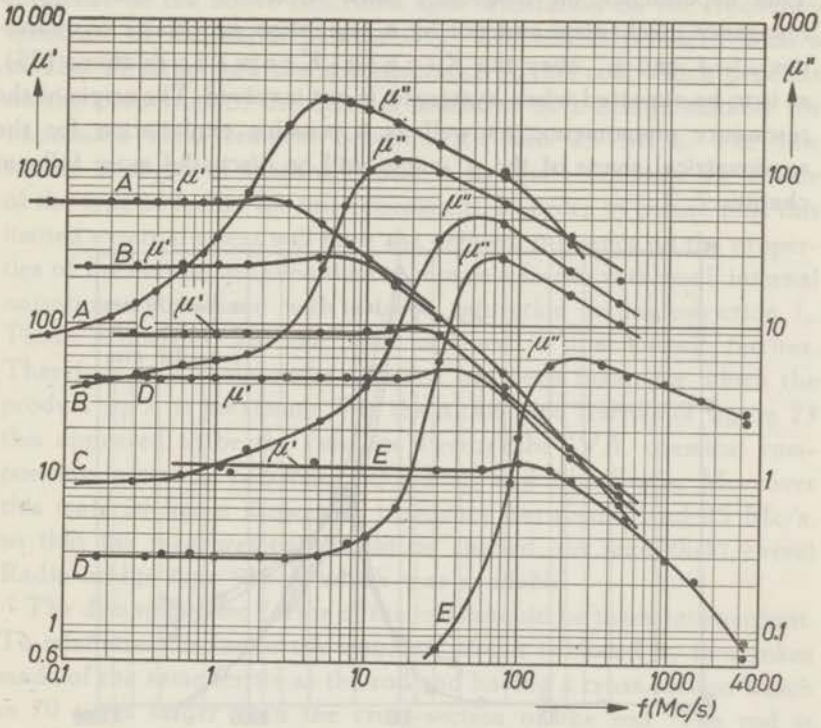

Fig. 23. The real and imaginary part of the initial permeability, μ' and μ'' respectively, as a function of frequency for samples of nickel zinc ferrite with various nickel zinc ratios, see table III. Note the different scales for μ' and μ''.

constant. For Ferroxcube IV*E* the measurements have been carried out up to 3160 Mc/s and the results are also represented on another scale in figure 24. Brockman, Dowling and Steneck (34) found that in ferrites dimensional resonances can occur if as a consequence of high permeability and high dielectric constant, the electromagnetic wave length in the material has the order of magnitude of the smallest dimension of the sample. For Ferroxcube IV*E* ($\varepsilon = 15$ above 10 Mc/s) this effect can influence the measuring results only above 1000 Mc/s when the smallest ring dimension is 5 mm. Nevertheless at each frequency rings with

different heights have been measured, so as to be sure that dimensional effects do not influence the results.

In this case the quantity $\mu'-1$ shows also a small maximum before it drops to low values, and at 3000 Mc/s it has a negative value. This dependence on frequency must therefore be caused by a resonance mechanism and not by a relaxation process. The quantities $\mu'-1$ and μ'' obey the Kronig-Kramers relations (35), as is to be expected when hysteresis is not involved. The origin of the resonance phenomenon as well as a possible explanation for the asymmetrical shape of the μ''-curve will be discussed more fully in chapter 7. 2.

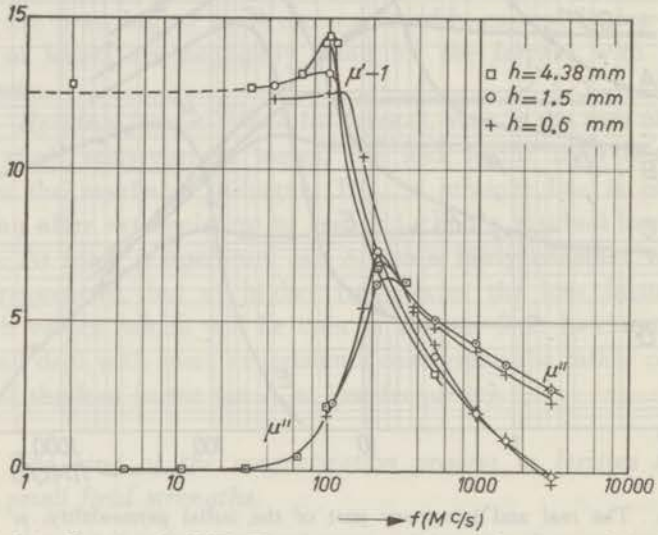

Fig. 24. Ferroxcube IV*E*. The quantities $\mu'-1$ and μ'' as a function of frequency.

5. 2. 2. The influence of externally applied mechanical stresses on the frequency *spectrum* of the initial permeability.

In order to find the origin of resonance described in the preceding chapter, it is of interest to know the frequency *spectrum* of the initial permeability of ferrites for which it is known beforehand that the magnetization is merely brought about by wall displacements or by rotations in unison of the spins in each Weiss domain. In chapter 4. 3 it is seen that this can be realized in ferrites under externally applied mechanical stress. A sufficiently high external tensile stress will force the magnetic spins in the Weiss domains

to be directed perpendicularly to the axis of the rod. Consequently an external field parallel to the axis of the rod exerts no force on the domain walls. As it is difficult to apply the required stress to rings of ferrite, a thin rod *) of ferrite is used to measure the influence of the above described spin orientation on the frequency *spectrum* of the initial permeability. The rod is provided with a number of turns, and the selfinductance of this coil, which depends on the properties of the core, is measured in a bridge suitable for impedance measurements between 0.4 and 25 Mc/s. The low tensile strength of ferrites (about 4 kg/mm^2) restricts the choice of the type of ferrite for this experiment. In order to ensure that this limited external stress will have the greatest influence on the properties of the ferrite, we should have chosen a ferrite with small internal anisotropies combined with a large saturation magnetostriction λ_s. These properties are not met together in the known ferrites. Therefore as a compromise a ferrite has been taken for which the product $\mu_0 . \lambda_s$ is maximum. For the nickel zinc ferrites of figure 23 this appeared to be the case for Ferroxcube IV*A*, chemical composition in mol % 17.5 NiO, 33.2 ZnO and 49.3 Fe_2O_3. Moreover this material has a dispersion frequency between 1 and 25 Mc/s, so that the measurements could be carried out with the General Radio bridge type 916-A which was available.

The demagnetizing factor of the rods should be taken into account. To minimize this factor the magnetic circuit is closed by two yokes made of the same ferrite as the rod and having a cross-section which is 70 times larger than the cross-section of the rod. The rod is

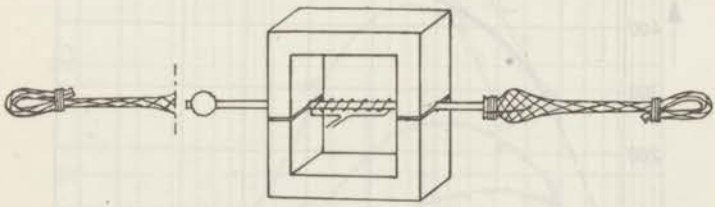

Fig. 25. Device to minimize the demagnetizing factor of a rod-shaped core.

ground accurately into the yokes to obtain a very small air gap, see figure 25. The ratio of the cross-sections of yoke and rod being great, only a small correction for the magnetic resistance of the

*) It must be borne in mind that these rods have been formed by an extrusion process while the rings were always formed by pressing. Some properties which are irrelevant for the following may therefore be different (36).

yoke is necessary. To apply the external stress, a lump of "Araldite" is melted on to each end of such a rod. Over the lump a flexible metal shield is forced as depicted in figure 25.

First of all the value of the stress has been determined for which it can be expected that mainly the rotation processes contribute to the magnetization in the axial direction of the rod. B e c k e r (37) calculated that for nickel under tensile stress the initial permeability μ_0 at sufficiently large values of the externally applied stress σ_e is given by the relation

$$\mu_0 = \frac{4\pi I_s^2}{3\sigma_e} \cdot \overline{\lambda_s^{-1}}, \qquad [18]$$

where $\overline{\lambda_s^{-1}}$ is the mean of the reciprocal value of the magnetostriction in the different crystal directions. This relation holds when the magnetostriction is negative, μ_0 is measured in the direction of the applied stress and domain-wall displacements do not occur. In the case of ferrites under tensile stress, the porosity of the material must be taken into account, and the correct formula reads

$$\mu_0 = \frac{4\pi I_s^2}{3\sigma_e} \left(\frac{d_x}{d}\right)^{1/3} \cdot \overline{\lambda_s^{-1}}, \qquad [19]$$

where d and d_x are the apparent density and the X-ray density of the ferrite respectively. In accordance with formula [19] the quantity μ_0 of Ferroxcube IV*A* has been plotted in figure 26 against

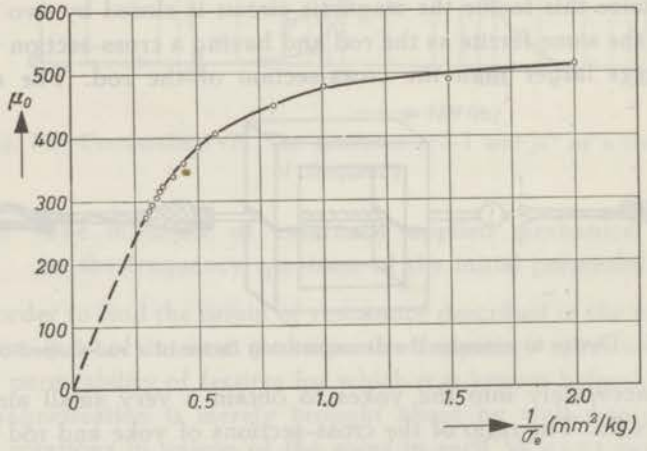

Fig. 26. The initial permeability μ_0 of a rod of the nickel zinc ferrite Ferroxcube IV*A* (chemical composition in mol % 17.5 NiO, 33.2 ZnO and 49.3 Fe_2O_3) as a function of externally applied tension σ_e.

the reciprocal value of the applied stress. It can be seen that from about $\sigma_e = 2.7$ kg/mm^2 onwards the relation [19] is obeyed. From the slope of the straight line a value for $1/\overline{\lambda_s^{-1}}$ can be calculated: $I_s = 292$ Gauss, $d = 4.90$ and $d_x = 5.35$, from which follows $1/\overline{\lambda_s^{-1}} = 5.0 \times 10^{-6}$. This value must be compared with the mean value of the magnetostriction that is known from the length variation measured for a rod of the same material in a magnetic field: $\lambda_s = 3.7 \times 10^{-6}$. The difference between both values is a consequence of the different values of the magnetostriction in different crystal directions. (This anisotropy has been measured for magnetite (38)).

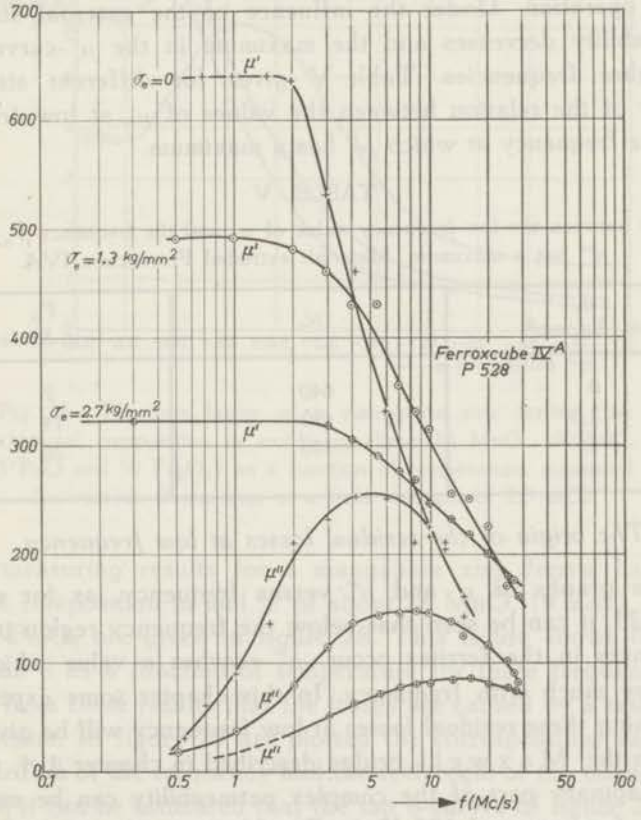

Fig. 27. The real and imaginary part of the initial permeability, μ' and μ'' respectively, plotted against frequency for different values of externally applied tension σ_e. The ferrite is the same as that of figure 26.

It can therefore be concluded that for tensile stresses of this order of magnitude and higher, the initial permeability depends merely on σ_e and no longer on the internal stresses, the crystal anisotropy or internal demagnetization. The conditions have then been obtained that for magnetic fields directed along the axis of the rod, μ_0 depends on rotation processes only. The results of the measurements of the dispersion in the initial permeability of Ferroxcube IV*A* at different values of the externally applied tensile stress are given in figure 27. For $\sigma_e = 0$ the μ' and μ'' *versus* frequency curves for this rod produced by an extrusion process are quite similar to those given in figure 25 for a ring of the same chemical composition, but produced by a pressing process preceding the firing operation. Under the influence of the external stress the permeability decreases and the maximum in the μ''-curves shifts to higher frequencies. Table V gives for different stresses a survey of the relation between the values of μ_0 at low frequency and the frequency at which μ'' has a maximum.

TABLE V

Relation between the low-frequency value of μ_0 and the frequency f'_0 at which μ'' has a maximum. Material: extruded Ferroxcube IV*A*.

σ_e in kg/mm²	μ_0	f'_0 in Mc/s
0	640	7
1.3	490	14
2.7	320	26

5. 3. *The origin of the residual losses at low frequency.*

From graphs of μ' and μ'' versus frequency, as for example figure 23, it can be seen that below the frequency region in which resonances in the ferrites occur, μ'' reaches a value which does not vary much with frequency. In this chapter some experiments concerning these residual losses at low frequency will be given.

With the Maxwell bridge described in chapter 4. 4, the real and imaginary part of the complex permeability can be measured up to a frequency of 100 Kc/s. For ferrites with widely differing compositions these quantities have been measured as a function of temperature at the four fixed frequencies of 2, 8, 25 and 100 Kc/s. The measuring procedure is that the ferrite ring core is placed in a

copper block having a large heat capacity. This block is placed in a Dewar vessel and cooled to liquid nitrogen temperature. The copper block is heated to room temperature by a heating element. This heating is interrupted by periods during which a temperature equilibrium is obtained and the quantities μ' and μ'' are measured. In most cases the magnetic field strength used is 2.5 mOe. The temperature is measured with a silver-constantan thermocouple having a thickness of 200 microns and being welded on a copper plate that is inserted in the copper block, near the ferrite ring.

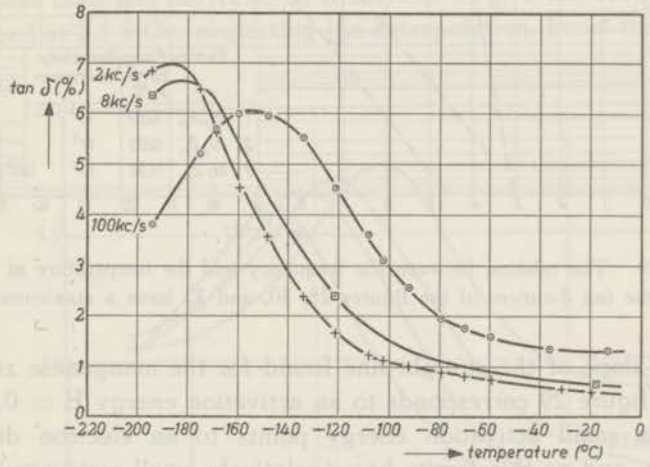

Fig. 28. The loss factor of a manganese zinc ferrite (the chemical composition in mol % is about 28 MnO, 19 ZnO, 3 FeO and 50 Fe_2O_3) as a function of temperature, measured for various frequencies at a field strength of 2.5 mOe.

The measuring results for a manganese zinc ferrite having a chemical composition in mol % of about 28 MnO, 19 ZnO, 3 FeO and 50 Fe_2O_3 are given in figure 28. This figure shows the loss factor tan δ as a function of temperature for three frequencies. It is clear from these results that the losses are caused by a relaxation phenomenon. In figure 29 are plotted the corresponding values of the logarithm of the frequency and the reciprocal of the temperature at which it can be estimated that the tan δ-curves of figure 28 have a maximum. The relation between both can be described by the general relaxation formula

$$\tau = \tau_\infty \, e^{\frac{E}{kT}} , \qquad [20]$$

where τ is the reciprocal of the angular frequency, T is the absolute temperature and E the activation energy of a relaxation process.

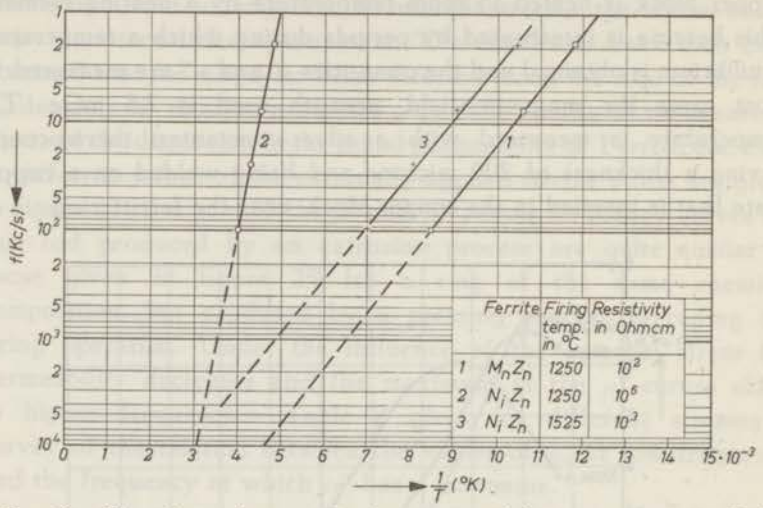

Fig. 29. The relation between the frequency and the temperature at which the tan δ-curves of the figures 28, 30, and 32 have a maximum.

The slope of the straight line found for the manganese zinc ferrite in figure 29 corresponds to an activation energy E = 0.11 eV. As this small activation energy points to an electron diffusion process, and as this ferrite has a relatively small resistivity (about 10^2 Ohmcm), the same kind of measurements has been carried out for a ferrite with a high resistivity, namely a nickel zinc ferrite, having before firing the chemical composition in mol %: 25 NiO, 25 ZnO and 50 Fe_2O_3 and being fired in oxygen at 1250° C (resistivity $\varrho = 10^6$ Ohmcm). The results are given in figure 30. It can be seen that in the temperature range covered tan δ is not a constant but the high values observed for the loss factor of the manganese zinc ferrite do not occur here. The variations in tan δ can again be ascribed to a relaxation process, and the corresponding values of the logarithm of the frequency and the reciprocal of the temperature at which the tan δ-curves for this ferrite have a maximum are therefore also plotted in figure 29. An activation energy is calculated of 0.41 eV. Afterwards this ferrite has been refired in the same atmosphere but at a higher temperature, 1525° C, thereby introducing 0.4% by weight of ferrous ions in the ferrite, which causes a decrease of the resistivity from 10^6 to 10^3 Ohmcm.

As we have seen in chapter 3. 2. 2, after firing at such a high temperature this ferrite causes already at low field strengths a high distortion, which means that hysteresis is important. Therefore μ' and μ'' of this ferrite have been measured at field strengths of 5 and 2.5 mOe so that an extrapolation to zero field strength can be carried out. The values of μ'' measured at these field strengths for 2, 8, 25 and 100 Kc/s are plotted against temperature in figure 31. After a linear extrapolation *) to zero field strength, the drawn lines are obtained. The variation of μ' with the field strength proved to be less than one per cent, so it suffices to give the values of μ' measured at 2.5 mOe, neglecting the extrapolation. From the values

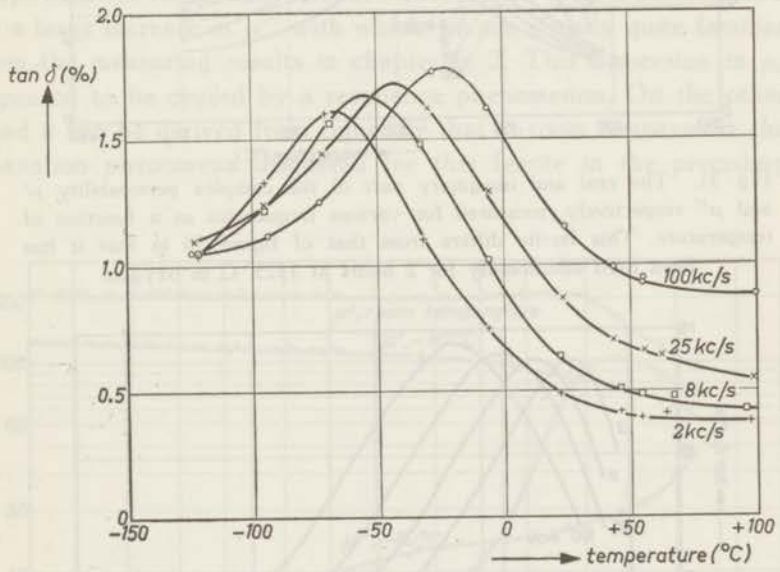

Fig. 30. The loss factor of a nickel zinc ferrite (before firing at 1250° C in oxygen its chemical composition in mol % was about 25 NiO, 25 ZnO and 50 Fe_2O_3) as a function of temperature, measured at a field strength of 2.5 mOe.

of μ' and the extrapolated values of μ'' a residual loss factor tan δ_r has been calculated; the result is given in figure 32, which shows the temperature dependence of tan δ_r for various frequencies. It can be seen that similar results are obtained as for the manganese zinc

*) This linear extrapolation is in accordance with equation [14].

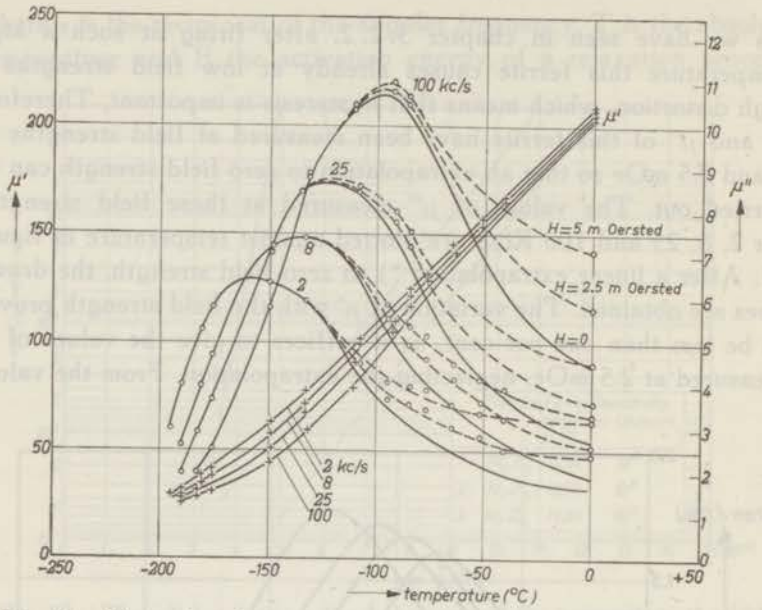

Fig. 31. The real and imaginary part of the complex permeability μ' and μ'' respectively, measured for various frequencies as a function of temperature. This ferrite differs from that of figure 30 in that it has been fired additionally for 2 hours at 1525° C in oxygen.

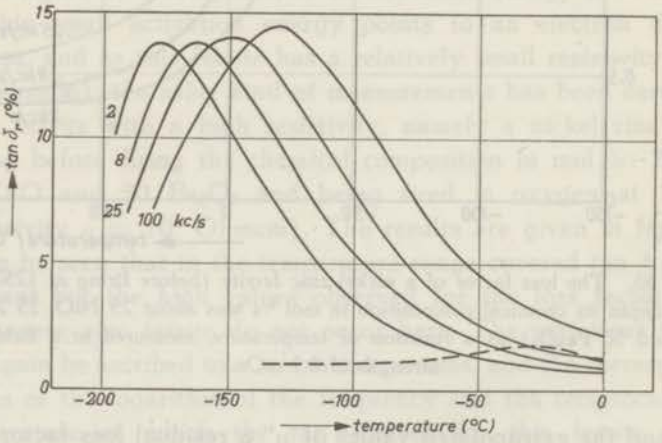

Fig. 32. The residual loss factor of the nickel zinc ferrite of figure 31 as a function of temperature. This ferrite has been fired at 1525° C, and has a resistivity of 10^3 Ohmcm. For comparison the dotted curve gives the loss factor at 100 Kc/s of the similar ferrite being fired at 1250° C and having a resistivity of 10^6 Ohmcm (This dotted curve is reproduced from figure 30).

ferrite which also contains both ferric and ferrous ions. Also the activation energies of the relaxation processes in both ferrites are the same (see figure 29).

5. 4. *An experiment showing both a resonance and a relaxation phenomenon in a ferrite.*

At room temperature the real and complex part of the initial permeability have been measured of that nickel zinc ferrite of chapter 5. 3, that was fired at 1525° C and that contains therefore both ferrous and ferric ions. The measuring results are represented in figure 33. The initial permeability of this ferrite is 210 and it drops to lower values above about 5 Mc/s. This drop is accompanied by a large increase in μ'', with which we are already quite familiar from the measuring results in chapter 5. 2. This dispersion in μ_0 appeared to be caused by a resonance phenomenon. On the other hand it can be derived from figure 29 that at room temperature the relaxation phenomena discussed for this ferrite in the preceding

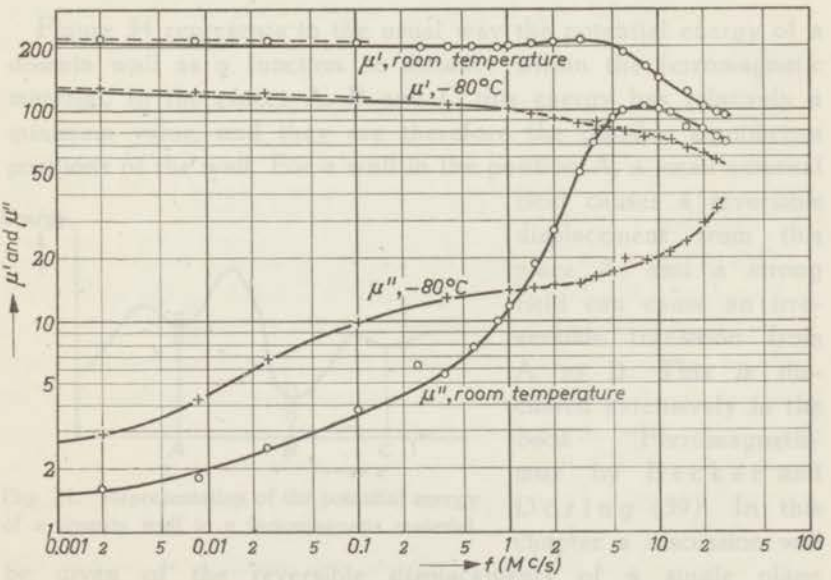

Fig. 33. The real and complex permeability of a nickel zinc ferrite at room temperature and at —80° C. (The chemical composition in mol % before firing at 1525° C in oxygen is 25 NiO, 25 ZnO and 50 Fe_2O_3).

chapter will also give rise to losses at about 5 Mc/s. These losses are obfuscated by the resonance losses (and they are perhaps partly responsible for the asymmetrical shape of the μ''-curve). At a lower temperature the anisotropy forces in the ferrite are greater (μ_0 decreases with temperature, see figure 2) and it may be expected that the resonance phenomenon is shifted to higher frequencies. On the other hand the relaxation frequency decreases with temperature and we must therefore expect that at a temperature which is sufficiently low, both dispersion regions have shifted considerably in opposite directions so that they can be distinguished clearly. In fact this proved to be the case at —80° C, as is shown in figure 33. It is obvious from the μ'' *versus* frequency curve at low temperature that two dispersion regions occur. We recognize the relaxation phenomenon at a frequency of about 1 Mc/s, and the resonance phenomenon above 20 Mc/s. The small increase of $\tan \delta$ found by Snoek (13) in some copper ferrites at low frequency might be explained along the same lines.

6. REVIEW OF THE MECHANISMS OF DISPERSION FOR THE INITIAL PERMEABILITY OF FERROMAGNETIC MATERIALS

6. 1. *Introduction.*

In the foregoing chapters it was found that in magnetizing ferrites the contribution of the various magnetization processes depends on the frequency used. Therefore in this chapter we will deal with the resonance and relaxation mechanisms for spin rotations and domain-wall displacements that have been discussed in literature.

Desaccomodation and after-effect with relatively a high time constant (greater than 1 sec.), which have also been observed (13) in ferrites, will not be considered.

6. 2. *Dispersion mechanisms for domain-wall displacements.*

Figure 34 represents in the usual way the potential energy of a domain wall as a function of distance within the ferromagnetic material. In the places A, B and C this energy has relatively a minimum value, and they are therefore the possible equilibrium positions of the wall. For a wall in the position A, a small external field causes a reversible displacement from this place A, and a strong field can cause an irreversible transition from A to B. This is discussed extensively in the book "Ferromagnetismus" by Becker and Döring (39). In this chapter a discussion will be given of the reversible displacements of a single plane domain wall in an infinite ferromagnetic material, thus excluding any boundary conditions. Döring (40) characterises such a wall by an equivalent mass m_w per cm^2, a friction coefficient β

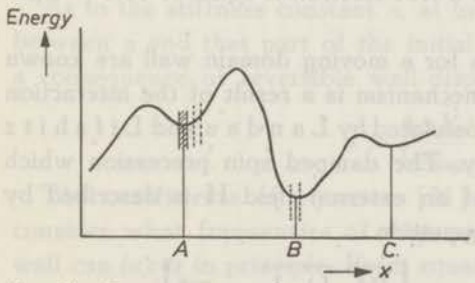

Fig. 34. Representation of the potential energy of a domain wall in a ferromagnetic material.

and a stiffness constant α. The equation of motion of this wall reads:

$$m_w\ddot{x} + \beta\dot{x} + \alpha x = c \,.\, I_s \,.\, H. \qquad [21]$$

The right hand term denotes the pressure exerted on the domain wall by an external magnetic field H, I_s is the saturation magnetization of the material, and c is a constant between 1 and 2, dependent on the kind of domain wall under consideration.

Equation [21] can be derived in the following way. Landau and Lifshitz (41) have shown that when a domain wall moves under the influence of an external magnetic field, in this moving wall a field must be present normal to this wall. The latter field must be strong enough to rotate the spins with the appropriate velocity over a conical surface from their direction in the decreasing adjacent Weiss domain to that of the growing one. Döring (40) pointed to the fact that as a consequence of this field, the wall energy of the moving wall is higher than that of the wall at rest. This additional energy can be regarded as kinetic energy of the moving wall, and an apparent mass m_w can be ascribed to the wall. This wall mass m_w for a uniform motion has been calculated by Döring (40) and in a simpler way by Becker (42). For a wall oscillating with a frequency smaller than the ferromagnetic resonance frequency (see chapter 6. 3), Rado (43) finds the same result:

$$m_w = \frac{1}{8\pi\gamma^2\delta}, \qquad [22]$$

where δ is the thickness of the domain wall and γ is the magneto-mechanical ratio*), which for a free electron is equal to 17.6 Mc per sec. Oersted.

Two damping mechanisms for a moving domain wall are known in literature. One damping mechanism is a result of the interaction between moving spins, first postulated by Landau and Lifshitz (41) in rather a formal way. The damped spin precession which starts under the influence of an external field H is described by these authors by the vector equation

$$\frac{d\vec{I_s}}{dt} = \gamma\left[\vec{I_s}\times\vec{H}\right] - \lambda\left[\frac{(\vec{H}\,.\,\vec{I_s})\,.\,\vec{I_s}}{I_s^2} - \vec{H}\right], \qquad [23]$$

*) When the spin rotations are damped, the quantity γ in equation [22] should after Kittel (44) be replaced by γ^*,

$$(\gamma^*)^2 = \gamma^2 + \frac{\lambda^2}{I_s^2},$$

where λ is the damping coefficient introduced in formula [23].

where the first term on the right represents the precession of a spinning top and the second term the damping of this precession determined by a constant λ, causing the spins to be oriented ultimately into the direction of the field H. With this damping coefficient λ for rotating spins is intimately related a friction coefficient β for a moving domain wall. The relation between both has been given explicitly by Kittel (44):

$$\beta_{\text{Kittel}} = \frac{\lambda}{2\gamma^2\delta} . \qquad [24]$$

A second friction mechanism for a moving wall is caused by the micro eddy-currents that are induced when in the wall $\operatorname{div} \vec{I} \neq 0$. Becker (45) has calculated this friction for the very improbable case that in the domain wall $\operatorname{div} \vec{I} = 2I_s$. However, it is known now (46) that in an ideal ferromagnetic material the normal component of the magnetization through the wall is constant. Deviations from this rule can be caused by strain and shape anisotropies in the material. Therefore the result of Becker's calculation gives a maximum value for the friction coefficient β caused by micro eddy-currents:

$$\beta_{\text{Becker}} = \pi^2 \cdot I_s^2 \, \frac{l\sigma}{c^2} . \qquad [25]$$

In this equation l denotes the mean distance between the domain walls, σ the electric conductivity of the material and c the velocity of light.

As to the stiffness constant α, at low frequency a relation exists between α and that part of the initial permeability, μ_{displ}, which is a consequence of reversible wall-displacements:

$$\alpha = \frac{4\pi I_s^2}{l\,\mu_{\text{displ}}} . \qquad [26]$$

The coefficients of equation [21] being determined, we shall consider what frequencies of dispersion for an oscillating domain wall can occur in principle. From equation [21] follows a resonance frequency ω_0 and a relaxation frequency ω_1 given by the formulae

$$\omega_0 = \sqrt{\frac{\alpha}{m_w}} \quad (\text{if } \beta^2 << \alpha m_w) , \qquad [27]$$

and

$$\omega_1 = \frac{\alpha}{\beta} \quad (\text{if } \beta^2 >> \alpha m_w) . \qquad [28]$$

By using the relations [22], [24], [25] and [26] we find for reversible domain-wall displacements the resonance frequency (42)

$$\omega_0 = \frac{4\pi\gamma I_s}{\sqrt{\mu_{\text{displ}}}} \cdot \sqrt{\frac{2\delta}{l}}, \qquad [29]$$

and the relaxation frequencies, according to Landau and Lifshitz (41) and Kittel (44)

$$\omega_{1\ \text{Kittel}} = \frac{8\pi\gamma^2\delta I_s^2}{\lambda l \mu_{\text{displ}}}, \qquad [30]$$

and according to Becker (42)

$$\omega_{1\ \text{Becker}} = \frac{4c^2}{\pi l^2 \sigma \mu_{\text{displ}}}. \qquad [31]$$

6. 3. *Dispersion mechanism for spin rotations.*

The possibility of a resonance of the electron spin of a ferromagnetic material was predicted theoretically in the above mentioned article by Landau and Lifshitz (41). Griffiths (47) using thin nickel layers was the first to find this ferromagnetic resonance in an external field. After that the ferromagnetic resonance phenomenon has been discussed extensively by numerous authors (48, 49, 50) and it has first been dealt with for ferrites by

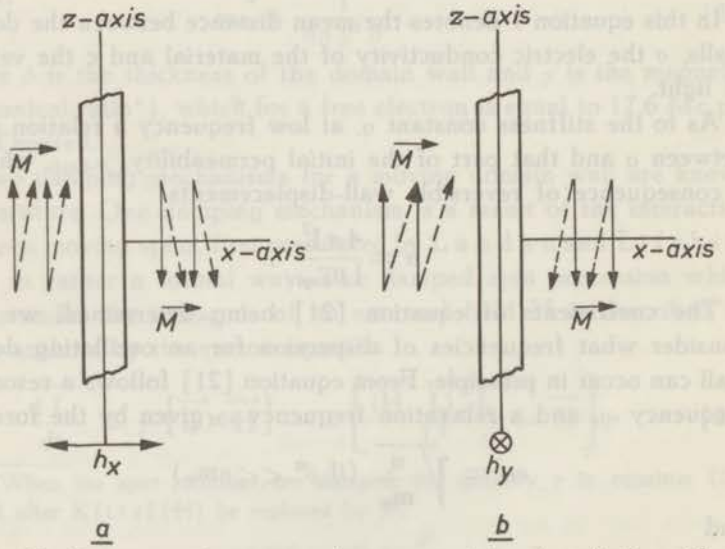

Fig. 35. Ferromagnetic resonance phenomena and domain walls. h_x and h_y are the external alternating field and $\vec{M}$ is the magnetic moment of a spin.

Snoek (51). Snoek's equation for the natural ferromagnetic resonance frequency ω'_o in a cubic polycrystalline material is

$$\omega'_o \cdot (\mu_{rot} - 1) = \frac{8\pi}{3} \gamma I_s, \qquad [32]$$

where μ_{rot} denotes the permeability of the material as far as it is brought about by rotations in unison of the spins in a Weiss domain. An extension of equation [32] has been suggested by Polder (52) and more quantitatively by Polder and Smit (53). The simple equation suggested by Snoek applies to the case of figure 35 a, where the external alternating field is perpendicular to the domain wall. However, this equation should be altered for the configuration of figure 35 b, where the alternating field is parallel to the domain wall. According to Polder and Smit, the resonating spins of the Weiss domains in figure 35 b will induce alternating magnetic charges on the interjacent domain wall, corresponding with a virtual demagnetizing field. Neglecting damping this can be understood easily from the equation of motion for spins with a magnetic moment $\overrightarrow{M}$ in an external field $\overrightarrow{H}$:

$$\dot{\overrightarrow{M}} = \gamma \left[\overrightarrow{H} \times \overrightarrow{M}\right] . \qquad [33]$$

When in figure 35 b the z-axis is taken parallel to $\overrightarrow{M}$ and the x-axis perpendicular to the 180°-domain wall, one of the equations [33] for a sinusoidal field $\overrightarrow{H}$ is

$$i\omega M_x = \gamma H_y M_z, \qquad [34]$$

and it can be seen easily that magnetic poles are induced in the wall as a consequence of the spin precessions in the adjacent Weiss domains. These wall effects can cause an important broadening or a displacement of the natural ferromagnetic resonance curve to higher frequencies. For it are the alternating magnetic charges on the domain walls and on the boundaries between the ferromagnetic material and another phase (e.g. air) that will cause stray fields in the Weiss domains, giving thus rise to an increase of the resonance frequency. The highest resonance frequency to be expected for an isolated homogeneously magnetized ellipsoid follows from the general ferromagnetic resonance formula given by Kittel (48),

$$\omega = \gamma I_s \sqrt{(N_x - N_y)\ (N_z - N_y)}, \qquad [35]$$

where N_x, N_y and N_z are the demagnetizing coefficients in the x, y and z direction respectively. Since the sum of these coefficients

equals 4π, the maximum resonance frequency that can be expected is

$$\omega_{max} = \gamma \cdot 2\pi I_s \,. \qquad [36]$$

However, in special configurations the resonance frequency can be twice as high as that given by equation [36]. This has been found experimentally by Beljers, van der Lindt and Went (36), and has been discussed theoretically by Polder and Smit (53).

7. DISCUSSION OF THE MAGNETIC DISPERSIONS FOUND IN FERRITES

7.1. *Discussion of the relaxation of the irreversible domain-wall displacements.*

From the measuring results given in chapter 3 it is evident that in general the permeability μ of a ferrite depends on the amplitude and the frequency of the externally applied sinusoidal magnetic field *). The points in figure 36 show the frequency dependence of μ for some ferrites of table II on a relative scale. These per-

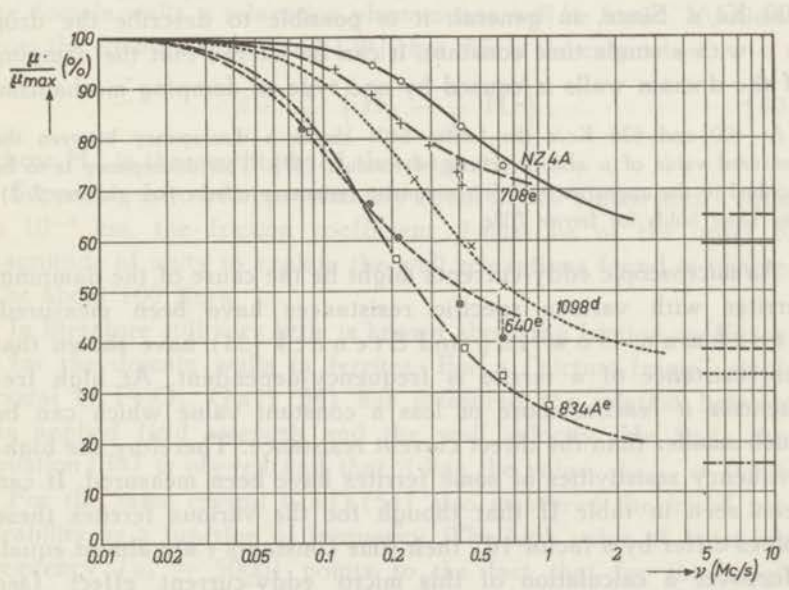

Fig. 36. The relative values of the permeability as a function of frequency for some ferrites of table II. Inserted points are interpolated measuring results; the lines are drawn according to formula [37] with a value of τ which fits best the measurements. (For ν read: f).

meabilities are defined as B/H for that value of the sinusoidal field strength at which the permeability at low frequency has a

*) The permeability μ is defined by the relation $B_{max} = \mu H_{max}$.

maximum. This field strength is chosen to ensure that the irreversible wall displacements which are under investigation, will relatively give the largest contribution to the magnetization.

The decrease of the permeabilities in figure 36 resembles very much that caused by a relaxation mechanism. Therefore in the same figure Debye curves have been drawn according to the formula

$$\mu = \mu_0 + (\mu_{max} - \mu_0) / \sqrt{1 + f^2\tau^2}, \qquad [37]$$

where μ_0 denotes the initial permeability, μ_{max} the maximum permeability at low frequency, f the frequency and τ a time constant which is chosen for each ferrite such that the curve [37] matches best the measured points. The reciprocal value of the time constant τ for the various ferrites is given in table II. They do not diverge very much for those ferrites for which they could be determined, and on the average they correspond with a frequency of about 100 Kc/s. Since, in general, it is possible to describe the drop in μ with a single time constant, it can be infered that the damping of the domain walls is caused by one type of damping mechanism.

At 400 and 626 Kc/s the ferrite 640e shows a discrepancy between the measured value of μ and the curve of formula [37]. This discrepancy is to be ascribed to the appearance of ferromagnetic resonance effects (see chapter 7.2). The same holds for ferrite 708e.

As microscopic eddy-currents might be the cause of the damping, ferrites with various specific resistances have been measured. Brockman, Dowling and Steneck (34) have shown that the resistance of a ferrite is frequency-dependent. At high frequencies it reaches more or less a constant value which can be much smaller than the direct current resistance. Therefore the high-frequency resistivities of some ferrites have been measured. It can been seen in table II that though for the various ferrites these values differ by a factor 10^6, their time constants τ are almost equal. Moreover a calculation of this micro eddy-current effect (see Becker (45) and formula [25] in chapter 6.2) results in a much higher relaxation frequency. A damping of the irreversible domain-wall displacements by eddy currents will not take place in these ferrites in the frequency range considered.

Relaxation of the irreversible domain-wall displacements means that a moving wall suffers a friction hindering it from covering the same distance in the short time available at high frequency, as would be the case at the same maximum field strength at low

frequency. Neglecting the wall mass *), the equation of motion of a 180°-wall reads

$$\beta \dot{z} = 2 I_s (H - H_c). \qquad [38]$$

Here it is supposed that very shortly after applying the field strength H the wall has the maximum velocity $\dot{z}$. H_c is the minimum value of the field strength for irreversible wall movements, it is of the order of magnitude of the coercive force of single crystals (32, 54). At a frequency f of the magnetic field the distance l over which an irreversible wall displacement can take place is:

$$l = \int_{t=0}^{t=\frac{1}{4f}} \dot{z}\, dt . \qquad [39]$$

When l is smaller than about half the average distance between the domain walls, a relaxation phenomenon will be found. It follows from the equations [38] and [39] that this is the case when

$$\beta \geq \frac{I_s}{lf} \left(H_m - \frac{\pi}{2} H_c \right), \qquad [40]$$

where H_m is the amplitude of the magnetic field.

Supposing I_s to be approximately equal to 300 Gauss and l equal to 10^{-3} cm, the friction coefficient β must be of the order of magnitude of unity to explain the wall relaxations found in chapter 3 at about 100 Kc/s.

In literature still very little is known about the friction coefficient β for the domain walls in ferrites. For a "picture-frame" single crystal of Fe_3O_4, Galt (54) has measured the relation between the applied field strength and the wall velocity. He finds that equation [38] is obeyed and that β has the value: $\beta_{Fe_3O_4} = 0.406$.

For the same crystal Galt (54) also measured the initial permeability as a function of frequency. The high value of μ_0 at low frequency ($\mu_0 \approx 5000$) points to the fact that for this single crystal the domain walls give the greater contribution to the permeability. These reversible domain-wall displacements have a relaxation frequency of 3000 c/s. Galt calculates with the aid of formula [28] a friction constant β which is nearly that given above. So it is reasonable that for the ferrites with a frequency-dependent

*) This is allowed for, since the mass of a domain wall will not cause a relaxation effect in the permeability that is brought about by irreversible domain-wall displacements.

magnetization curve, the quantity β has the order of magnitude of unity. On the other hand, from the known damping coefficient λ of nickel ferrite (55), we calculate with the aid of formula [24] a friction coefficient $\beta_{NiFe_2O_4} = 0.02$. From this low value follows a relaxation frequency for the irreversible wall-displacements of about 100 Mc/s, (taking $H_m - \frac{\pi}{2} H_c = 10$ Oersted), far beyond our measuring range. As it is found that the relaxation frequency shifts to higher values for ferrites with a lower initial permeability, we can conclude that β decreases with the permeability.

7. 2. *Discussion of the resonance phenomenon found for the initial permeability.*

In figure 23 the initial permeability of a series of sintered polycrystalline nickel zinc ferrites is given as a function of frequency. As we noticed earlier, these curves show the typical characteristics of a resonance phenomenon. For, apart from the small increase of μ' which in most cases is found before it drops to low values, a negative value of μ'—1 is measured at high frequency, *e.g.* at 3000 Mc/s for Ferroxcube IV*E*, see also figure 24. The question is, what does resonate here, or in other words, is the initial permeability of these ferrites mainly a result of reversible domain-wall displacements or a result of rotation processes? The resonance frequency will then be determined either by formula [29] or [32]. These formulae show a great difference as to the dependence of the resonance frequency on the value of the initial permeability. In the case of a wall resonance, the resonance frequency ω_o increases at most proportional to $1/\sqrt{\mu_o}$, for as a rule the thickness δ of the wall decreases with decreasing μ_o. On the contrary the ferromagnetic resonance frequency ω'_o is proportional to $1/\mu_o$ and a comparison of the measured resonance frequency with μ_o might give a decisive answer to the question formulated above.

The initial permeability corresponding, according to the ferromagnetic resonance equation [32], to the measured resonance frequency ω'_o is calculated in table VI. At the resonance frequency of a single resonance phenomenon the permeability has dropped to half its low-frequency value. In the polycrystalline ferrites a great number of resonances occur and in this case too the resonance frequency f'_o will be defined as the frequency where μ'—1 has dropped to half its low-frequency value. It appears from the two

last columns of table VI that a good agreement exists between the measured initial permeability and the permeability calculated from the ferromagnetic resonance frequency according to Snoek's relation [32].

TABLE VI

Comparison between the measured ferromagnetic resonance frequency and the initial permeability of mixed nickel zinc ferrites.

Ferroxcube*) IV	$f'_0 = \frac{\omega'_0}{2\pi}$ in Mc/s	I_s in Gauss	$\mu_{rot} - 1 = \frac{4\gamma \cdot I_s}{3f'_0}$	μ_0 measured
A	8	292	825	640
B	30	332	255	240
C	75	321	95	85
D	140	283	46	44
E	350	197	13	12

*) The chemical composition of these ferrites is given in table III.

Snoek's relation between the initial permeability and the resonance frequency still holds when for the latter is taken the frequency where the μ''-curve has a maximum. However, in this case the product of corresponding values is too small by about a factor 1.5.

When the dispersion region found in the *spectrum* of the initial permeability of ferrites is caused by a ferromagnetic resonance, it should still be present when wall displacements are inhibited and only spin rotations can occur. This has been found to be the case in a ferrite under a large tensile stress, as discussed in chapter 5. 2. 2. It is beyond doubt that the dispersion which is still found in the initial permeability in the case of a large stress $\sigma_e = 2.7$ kg/mm^2, see figure 27, is due to ferromagnetic resonances. Moreover, if Snoek's picture is correct, a simple relation must exist between the resonance frequencies found in the cases of $\sigma_e = 0$ and a high value of σ_e. Equation [32] applies to the first case, while in the second case a factor $^2/_3$ should be omitted on the right hand side. The values of μ_0 that have been measured at low frequency and the corresponding values of the frequency f'_0 at which μ_0 has dropped to half of its low-frequency value are given in table V for three values of σ_e. From the values of μ_0 and f'_0 measured without external stress, can be calculated a resonance frequency of 21 Mc/s for the case that μ_0 has decreased to 320 by the applied stress. This is to be compared with the resonance frequency of 26 Mc/s

which is actually found. The result is in reasonably good agreement with what is to be expected according to Snoek's picture.

These measuring results point to the fact that the initial permeability of these ferrites is mainly determined by a rotation in unison of the electron spins in a Weiss domain from their equilibrium position in the internal field into the direction of the applied magnetic field. Of course the comparison of f'_0 with μ'_0 given above, still admits the possibility that reversible wall-displacements give a minor contribution to the permeability. This refinement will not be considered here.

However, it remains unsatisfactory that on the one side the explanation of this dispersion is in good accordance with the experiments described in chapter 5.2, whereas on the other hand the μ_{rot} calculated for those ferrites for which the crystal anisotropy constant K_1 is known, is sometimes smaller than the measured one. From hysteresis loop measurements on a single crystal of nickel ferrous ferrite, Galt, Matthias and Remeika (56) find: $K_1 = -6.2 \times 10^4$ ergs/cm^3, and Yager, Galt, Merritt and Wood (55) find from ferromagnetic resonance experiments on a similar crystal, $K_1 = -6.27 \times 10^4$ ergs/cm^3. With these values corresponds a permeability of 10.4 if it is exclusively due to rotation processes. This value must be compared with $\mu_0 = 12$ for Ferroxcube IV*E* of table VI. But for a manganese zinc ferrite (chemical composition in mol % 23 MnO, 27 ZnO and 50 Fe_2O_3) Galt, Yager, Remeika and Merritt (57) find $K_1 = -3.8 \times 10^3$ ergs/cm^3, from which follows a permeability of 72, much smaller than what is found for the polycrystalline ferrite 708e of approximately the same chemical composition (see table II).

It follows from the shape of the μ'' *versus* frequency curve that the ferromagnetic resonances in the polycrystalline ferrites are spread over a large frequency range. Dependent on the type of the ferrite, the quantity μ'' increases rapidly at a frequency somewhere between 30 and 200 Mc/s, but it decreases slowly and at 3000 Mc/s it has still one third of its peak value. This might be explained by Polder and Smit's theory given in chapter 6. 3, *i.e.* the resonance frequency depends on both the internal anisotropy field and a virtual demagnetizing field, which is $4\pi I_s$ at maximum. The corresponding maximum frequency is quite near 6000 Mc/s. These authors also give an explanation for the fact that the maximum of the losses are found near the resonance frequency given bij Snoek's formula [32].

In chapter 6. 3 it has been shown that in ferromagnetic materials consisting of many Weiss domains, resonances can occur from the frequency ω'_0 up to $2\pi\gamma I_s$ and in special cases up to $4\pi\gamma I_s$. This is also found experimentally (fig. 23).

However, it appeared to be not the case for very small grains consisting of few or even a single Weiss domain.

A manganese zinc ferrite (chemical composition in mol % 27 MnO, 19 ZnO, 3 Fe_2O_3 and 50 Fe_2O_3) having an initial permeability of about 1000, and correspondingly a maximum in the ferromagnetic resonance losses at a frequency of 2 Mc/s, is ground to fine particles for 48 hours under alcohol in an agate ball mill. After that, the coarse and fine grains were separated by a simple sedimentation process. Though it is difficult to measure the dimensions of these magnetic particles, an estimation can be made with a microscope. The greater part of the grains have a diameter of about 1 micron. With a binder of stearic acid these grains are formed into a ring having an initial permeability of 12 and a magnetic saturation I_s of about 225 Gauss (I_s of the solid material is 375 Gauss). According to Snoek's formula the μ''-curve for the powdered ferrite should have a maximum at $\frac{1000}{12} \times \frac{225}{375} \times 2$ Mc/s, *i.e.* 100 Mc/s. Fig. 37 shows the measured curves for the complex permeability. The resonance phenomena occurring at about 2 Mc/s in the solid ferrite are now wholly absent and instead of these a new dispersion region is found at about 1000 Mc/s. Although one might be inclined to expect resonance frequencies below the values given by Snoek's formula, the resonance frequencies are actually much higher. This can be understood to some extent by supposing that the magnetically isolated particles consist of a very small number of Weiss domains so that the virtual charges which in massive ferrites will only in small regions give an increase of the resonance frequency, do give an additional field throughout the whole particle and a consequential shifting of the resonances to higher frequencies.

Similar measurements have been carried out by Rado et al. (58) on the sintered magnesium ferrite "Ferramic A". In this material two dispersion regions are found at 50 and 1500 Mc/s respectively. As the initial permeability is 18 the low frequency dispersion region can be explained according to Snoek. After powdering this ferrite into particles of 0.4 micron only one dispersion region is left at 2500 Mc/s. Therefore the authors ascribe the low-frequency dispersion to a domain-wall relaxation and the high frequency one to a ferromagnetic resonance of the spins. This argument however, is not conclusive and perhaps the extended theory of ferromagnetic resonance can give an interpretation of their results.

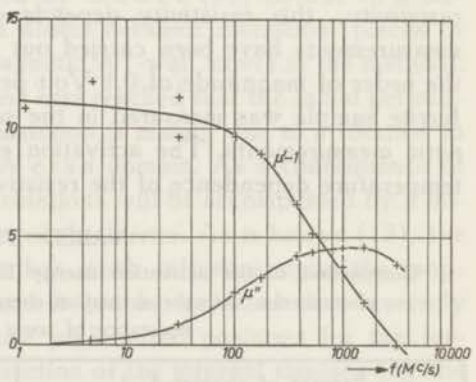

Fig. 37. Real and imaginary part of the initial permeability of a powdered manganese zinc ferrite. (Chemical composition in mol % 27 MnO, 19 ZnO and 50 Fe_2O_3; particle size about 1 micron).

7. 3. *Discussion of the relaxation phenomenon found for the initial permeability.*

In chapter 5. 3 a relaxation in the initial permeability of ferrites was found. The process has an activation energy of the order of a tenth of an electronvolt. A similar activation energy was found earlier by Verwey and Haayman (59) for the temperature dependence of the resistivity of Fe_3O_4 above the transition point, and by Verwey, Haayman and Romeyn (60) for the temperature dependence of the resistivity of some other spinels. Therefore, we have also measured the direct current resistivity of the ferrites of chapter 5. 3 as a function of temperature. For this purpose the ferrite ring was broken into two pieces. Both ends of one half of the ring were silvered. These ends served as current contacts. Two other silvered spots served as potential contacts. The potential measured across a part of the half ring was compared with the voltage drop across a known resistance carrying the same current as the ferrite. The voltages are measured with an electrometer, in order to ascertain that the internal resistance of the voltmeter is high compared with the resistances to be measured and also high compared with the resistance at the contacts. As it appeared that especially for the ferrites having a low direct-current resistivity, this resistivity depends on the voltage applied, the measurements have been carried out with low voltages, mostly of the order of magnitude of 0.1 Volt per cm. The temperature of the ferrite sample was measured in the same way as during the magnetic measurements. The activation energies E_ϱ derived from the temperature dependence of the resistivity of some ferrites are given

TABLE VII

Comparison of the activation energy E_M of the magnetic relaxation phenomenon with the activation energy E_ϱ of the direct current resistance of some ferrites.

Ferrites of chapter 5. 3		E_M in eV	E_ϱ in eV
Type	Resistivity at room temperature in Ohmcm		
MnZn	10^2	0.11	0.10
NiZn	10^6	0.41	0.37
NiZn	10^3	0.11	0.10

in the last column of table VII. The third column gives the activation energies E_M deduced from the magnetic loss measurements in chapter 5. 3.

In these cases a good agreement proves to exist between both activation energies and it is rather probable that the magnetic after-effect found in ferrites in which atoms of the same element occur as ions of two different valencies, is due to a diffusion process of electrons. The activation energy can be understood as the energy required for stripping an electron from a ferrous ion, which can be an ion on a tetrahedral or an octahedral lattice position.

The relaxation found by Galt, Matthias and Remeika (56) in the permeability of a single crystal of nickel ferrite has been ascribed by these authors to a relaxation of the reversible wall-displacements which determine the initial permeability of the single crystal to a large extent. From their measuring results an activation energy can be calculated which is about 0.2 eV. Since their single crystal contains many ferrous ions and shows a high electric conductivity, it is probable that the relaxation found by Galt et al. in this single crystal and the relaxation found by us in sintered ferrites are caused by the same mechanism. After-effects were found earlier by Richter (61) and Schulze (62) in carbonyl iron. This after-effect has been explained by Snoek (63) as due to a diffusion of carbon or nitrogen atoms between interstitial places of the iron lattice when a ferromagnetic 90°-wall moves in the material.

In chapter 7. 2 the conclusion was reached that the initial permeability of the ferrites under discussion is mainly due to a rotation in unison of the spins in each Weiss domain. As a consequence of the magnetostriction the spin rotations will be accompanied by a deformation of the crystal lattice of the ferrite. As is known (13), the concentration of ferrous ions has much influence upon the magnetostriction of the ferrite, and it can be expected that inversely the internal stresses will cause preferential positions for the ferrous ions. A change of the direction of the internal stresses (by the spin rotations) gives a redistribution of the ferrous and the ferric ions, which can simply be brought about by an electron diffusion.

8. TOTAL LOSSES AT HIGH ALTERNATING INDUCTIONS IN FERRITES

8.1. *Introduction.*

In chapter 5. 1 it has been discussed that a varying magnetic field in a ferrite core gives rise to electromagnetic losses, which are completely dissipated into heat. We will define the total losses in a ferrite core at a maximum induction B_{max} and a frequency f as the electromagnetic energy which in a previously demagnetized ferrite is dissipated into heat, when this ferrite is subjected to a sinusoidal magnetic field of frequency f causing in the ferrite a maximum induction B_{max}. At high amplitudes of the field strength these losses are at least partly due to irreversible domain-wall displacements occurring during magnetization. Now it has been found (chapter 7. 1) that for some ferrites at about 100 Kc/s and higher the contribution of these irreversible wall-displacements to the magnetization is reduced. Thus the losses involved will also decrease at a high frequency.

8.2. *Method of measuring the total losses.*

The total losses can be measured in two different ways. The phase angle δ between the induction and the field can be measured when a coil with the ferrite core is inserted in a bridge or resonance circuit, or the heat generated in the core can be measured with a calorimeter.

Phase angle measurements can be carried out very quickly, but the bridge circuit has the disadvantage that, at least in the bridges that are commercially available, the currents are limited to 30 mA. (*e.g.* the General Radio Bridge type 916 A) and the maximum voltage across the measuring coil is 10 Volt, so that high field strengths can not be obtained in the ferrite rings used.

There are two forms of the *resonance method:*

a. The quality factor Q is measured for a circuit consisting of a coil with the ferrite core under investigation and a capacitor having negligibly small losses ($Q = 1/\tan\delta$). This

method is useful if $Q > 10$ and it is therefore used for measuring low losses.

b. The known quality of a very sharp oscillating circuit ($Q > 500$) is lowered by inserting a small coil with ferrite core in series with the large coil. The quality change is a measure for the losses in the ferrite core (16). However, the ferrite core can cause a distortion in the voltage across the oscillating circuit, which leads to erroneous results.

On the other hand the *calorimetric method* is very simple and it permits the direct determination of the amount of energy which is dissipated into heat inside the ferrite core. We have therefore chosen this last method to measure the total losses of various ferrites as a function of maximum induction and frequency. The calorimeter of figure 38 consists of an unsilvered Dewar vessel containing olive oil, which gives very small dielectric losses (dielectric constant $\varepsilon \approx 3$). Metal parts are not used for the calorimeter to avoid heating by eddy currents generated by stray fields. The temperature is measured with a Beckmann thermometer. The heat capacity W of the calorimeter with accessories is determined from the temperature increase caused by a known direct current through a coil of resistance wire in the calorimeter. Determinations of W at different values of the direct current result in a mean value of $W = 73$ cal/degree, with an accuracy of 3%. The smallest heat generation that can still be measured with an accuracy of 10%, amounts to 20 mW. Copper losses proved to be of no importance. The circuit is that of figure 4 except for the secondary, which can be omitted. For the primary the conditions [6] and [7]

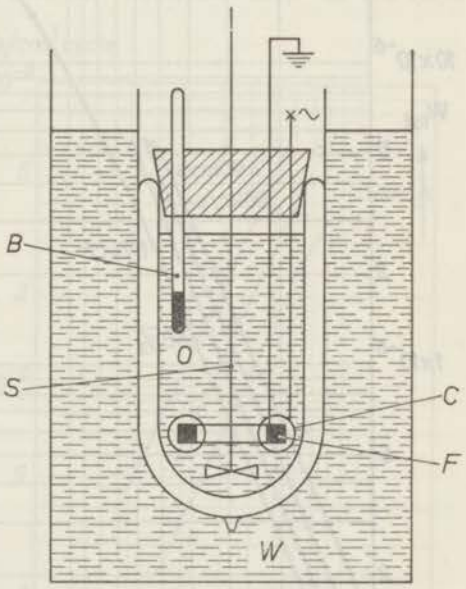

Fig. 38. The calorimeter. F ferrite core, C coil, S stirrer, B Beckmann thermometer, W water and O olive oil.

must be fulfilled. The total losses are measured as a function of frequency and maximum induction, the latter being determined from the measuring field strength and the previously measured magnetization curve of the ferrite.

8. 3. *Total losses measured with the calorimeter.*

With the calorimeter the total losses in some ferrites have been measured. The induction and frequency ranges covered are from 100 to 1000 Gauss and up to 500 Kc/s respectively. The upper limit is imposed by too great a heat being generated in the ferrite so that its temperature rise during the measurements is more than about 5 degrees Centigrade. We will give the measuring results separately for ferrites having a frequency-dependent and a frequency-independent magnetization curve according to chapter 3.

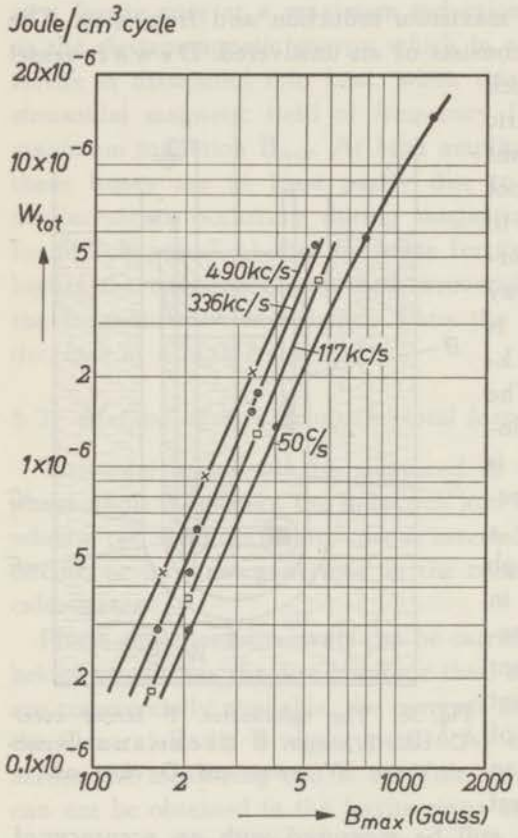

Fig. 39. Total losses at several frequencies as a function of B_{max} for ferrite 448Aa (see table II), which has a frequency-independent magnetization curve.

a) *Total losses of ferrites with a frequency-independent magnetization curve.*

Ferrite 448Aa of table II has a frequency-independent magnetization and distortion curve and it is therefore a suitable ferrite for measuring the total losses as a function of frequency. The resistivity of this material being 52 Ohmcm, eddy-current losses can be neglected if the smallest dimension of the sample per-

pendicular to the magnetic lines of force is some millimeters, as was actually the case. At low frequency, for instance at 50 c/s, the total losses are substantially caused by the irreversible domain-wall displacements. The area of the hysteresis loop at 50 c/s was determined by means of an integrating circuit and the result is given in the lowest curve of figure 39. Since for this ferrite the hysteresis loop closes at about 3000 Gauss, the loss per cycle still increases considerably with increasing induction at 1000 Gauss. In the same figure are given the total losses per cycle as determined with the calorimeter at 117, 336 and 490 Kc/s. It is evident that at all frequencies the losses depend in an analogous way on the induction ($W_{tot} \sim B_{max}^{2.4}$), and that for a given induction the loss per cycle increases with frequency. For this ferrite the distortion at 490 Kc/s is still the same as that at low frequency (see figure 13), so that the "hysteresis loop" at 490 Kc/s is formed by superposition of the low-frequency hysteresis loop and the ellipse corresponding to a phase shift between B and H determined by the additional loss per cycle at 490 Kc/s compared with those at 50 c/s. The cause of these additional losses is unknown but it might be that they are generated by the same mechanism which is found to be responsible for the residual losses in ferrites, *i.e.* an electron diffusion process (see chapter 7.3). The residual loss factor tan δ_r should than increase with the induction.

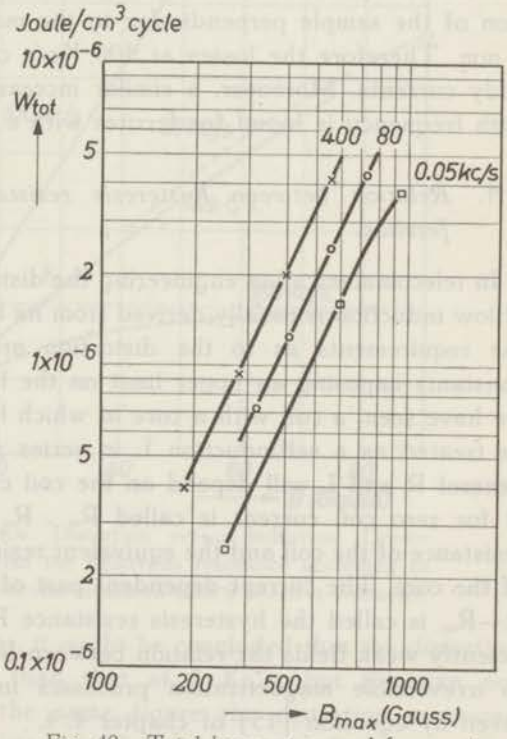

Fig. 40. Total losses at several frequencies as a function of induction B_{max} for ferrite 640e, which has a frequency-dependent magnetization curve.

b) *Total losses of ferrites with a frequency-dependent magnetization curve.*

As an example for this kind of ferrites the total losses are given for ferrite 640e (table II). The magnetization curves and the distortion at different frequencies are already known from the figures 10 and 11. From the results of the loss measurements given in figure 40 it appears that also in this case at constant induction the total losses per cycle increase with frequency, though at the same time the distortion decreases. The low-frequency hysteresis loop with sharp tips changes gradually into an ellipse at higher frequencies, which could also be verified on the screen of an oscilloscope. This ellipse corresponds with a phase shift δ between B and H. The loss factor tan δ which is determined by the total losses per cycle, is not a constant, but increases with B_{max}. The resistivity of this ferrite is 1.2 Ohmcm, and the smallest dimension of the sample perpendicular to the magnetic lines of force is 3 mm. Therefore the losses at 400 Kc/s can not be attributed to eddy currents. Moreover, a similar increase of the loss per cycle with frequency is found for ferrites with a much higher resistivity.

8.4. *Relation between hysteresis resistance and distortion in ferrites.*

In telecommunication engineering the distortion of a core material at low induction is usually derived from its hysteresis resistance and the requirements as to the distortion are always expressed in constants imposing an upper limit on the hysteresis resistance. As we have seen, a coil with a core in which losses are generated can be treated as a selfinduction L in series with a resistance R. In general R and L will depend on the coil current and the value of R for zero coil current is called R_0 . R_0 consists of the copper resistance of the coil and the equivalent residual loss resistance (28) of the core. The current-dependent part of the total resistance, *i.e.* $R—R_0$, is called the hysteresis resistance R_h of the core. For sufficiently weak fields the relation between R_h and the distortion due to irreversible magnetization processes in magnetic materials is given by equation [15] of chapter 4.4.

For the ferrites 640e and 834Ae (see table II) the hysteresis resistance R_h was measured at 2 Kc/s as a function of the induction in the core. The distortion calculated according to formula [15]

proved to be in agreement with the distortion measured at low frequency with a selective voltmeter (see figure 11 and the inset of figure 18 respectively).

At high frequencies relation [15] does not hold for ferrites, since the total losses per cycle increase at different frequencies with approximately the same power of the induction (see chapter 8. 3), and at a given value of B_{max} they increase with frequency. In agreement herewith the measured hysteresis resistance increases more than linearly with frequency, and according to formula [15], the calculated distortion would also increase with frequency. Figure 41 gives for instance the distortion calculated from the hysteresis resistance of ferrite 640e at 2 and 100 Kc/s.

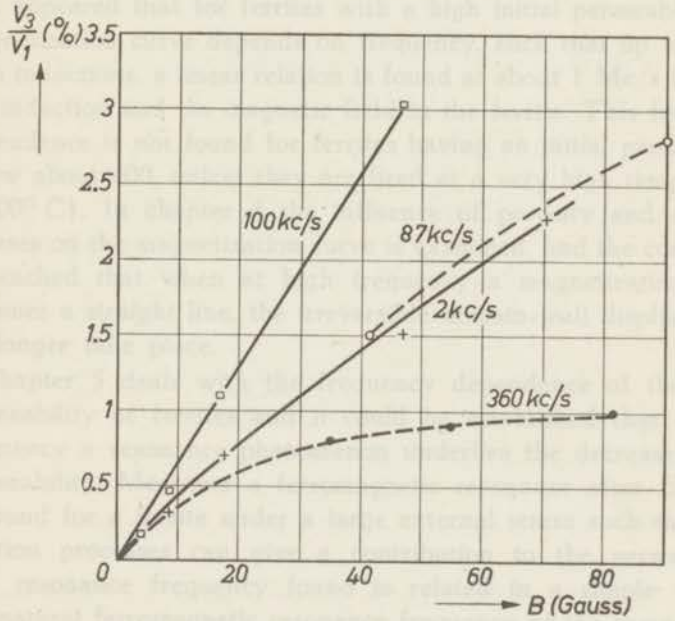

Fig. 41. Ferrite 640e. Distortion *versus* induction. Drawn curves: calculated from the hysteresis resistance according to formula [15]. Dotted curves: measured with a selective voltmeter.

From these calculations, it might be concluded that the distortion at 100 Kc/s is higher than that at 2 Kc/s, but this can not be true. Therefore in the same figure the distortion measured with the selective voltmeter at 87 Kc/s is given for comparison. As a consequence of the additional losses found in chapter 8. 3, the hysteresis resistance at high frequency cannot be considered

as a true measure for the non-linear behaviour of ferrites. If it is desired to know the distortion at high frequencies it must be measured directly, for instance with a voltage analyser. Deduction of the distortion from the hysteresis resistance measured at high or low frequency may give erroneous results.

SUMMARY

After a short review of the properties and the preparation technique of sintered ferrites, the measuring methods are described that have been used to determine the magnetization curves and the distortion as a function of frequency. A discussion is given of the conditions that must be fulfilled in order to limit the systematic error in the measuring results.

It appeared that for ferrites with a high initial permeability the magnetization curve depends on frequency, such that up to rather high inductions, a linear relation is found at about 1 Mc/s between the induction and the magnetic field in the ferrite. This frequency dependence is not found for ferrites having an initial permeability below about 400, unless they are fired at a very high temperature (1500° C). In chapter 4 the influence of porosity and external stresses on the magnetization curve is examined, and the conclusion is reached that when at high frequency a magnetization curve becomes a straight line, the irreversible domain-wall displacements no longer take place.

Chapter 5 deals with the frequency dependence of the initial permeability of ferrites and it could be established that at high frequency a resonance phenomenon underlies the decrease of the permeability. Moreover a ferromagnetic resonance after Snoek is found for a ferrite under a large external stress such that only rotation processes can give a contribution to the permeability. The resonance frequency found is related in a simple way to the natural ferromagnetic resonance frequency of the same ferrite. In this chapter are also given some results of measurements that point to a new relaxation phenomenon, which at least to a large extent is responsible for the residual losses in ferrites.

After having given in chapter 6 a brief survey of the theories found in literature concerning the dispersion mechanism of domain-wall displacements and spin rotations, the next chapter gives a confrontation of the measuring results with these theories. The following conclusions have been reached:

a. The relaxation of irreversible domain-wall displacements is

brought about by a friction process characterised by a friction coefficient having the order of magnitude of unity. The origin of this friction is unknown.

b. The theory of the ferromagnetic resonance permits many of the properties of the initial permeability at high frequency to be clarified.

c. The relaxation process causing at low frequency a dispersion in the initial permeability of ferrites, is closely connected with an electron diffusion. The activation energy of this relaxation process is the same as that found from the temperature dependence of the resistivity of ferrites.

Though in some ferrites at high frequency B is a linear function of H, it is seen in the last chapter that still many losses are generated in the ferrite giving rise to a phase shift between field and induction. Eventually it is discussed that in the case of ferrites the determination of the distortion from the hysteresis resistance can give erroneous results.

This work has been carried out in the Research Laboratories of the N.V. Philips' Gloeilampenfabrieken at Eindhoven. I am greatly indebted to the Directors of this laboratory as well as to many of my friends and colleagues for their helpful advice. I wish to remember that Dr J. J. Went introduced me into the field of ferromagnetism and that he was always a great help to me. Many discussions with Prof. Dr G. W. Rathenau and Ir J. Smit resulted in new experiments. Mr H. van der Heide assisted in acquiring a number of the measuring results.

SAMENVATTING

Na een kort overzicht van de algemene eigenschappen en de bereidingswijze der ferrieten, volgt een beschrijving van de meetmethodes die zijn gebezigd voor het bepalen van de magnetiseringskrommen en de vervormingen als functie van de frequentie. Uitvoerig is ingegaan op de voorwaarden die moeten worden gesteld opdat de systematische meetfout beneden een vooraf vastgestelde maximale waarde blijft.

De magnetiseringskromme van ferrieten met een hoge aanvangspermeabiliteit blijkt sterk van de frequentie af te hangen, en wel op een zodanige wijze dat tot tamelijk hoge inducties reeds bij een frequentie van ongeveer 1 MHz een lineair verband bestaat tussen de inductie en de magnetische veldsterkte in het ferriet. Deze dispersie wordt niet gevonden voor ferrieten met een aanvangspermeabiliteit beneden ongeveer 400 tenzij zij worden gebakken bij een zeer hoge temperatuur (1500°C). In hoofdstuk 4 wordt de invloed van de porositeit en van uitwendige krachten op de magnetiseringskromme onderzocht. Dit onderzoek leidt tot de conclusie dat de irreversibele verschuivingen der B l o c h-wanden in sommige ferrieten bij hoge frequenties niet of slechts gedeeltelijk plaatsvinden, zodat de magnetiseringskromme van de frequentie afhangt.

In hoofdstuk 5 wordt nog eens ingegaan op het frequentie*spectrum* van de aanvangspermeabiliteit van ferrieten. Door dit *spectrum* te meten tot 3000 MHz kon worden aangetoond dat de door S n o e k gevonden en verklaarde dispersie in μ_0 bij hoge frequentie, wordt veroorzaakt door een resonantie-proces. Bovendien blijkt een ferromagnetische resonantie volgens S n o e k op te treden in een ferriet onder een zodanig uitwendig aangelegde mechanische kracht, dat wandverschuivingen niet tot de permeabiliteit kunnen bijdragen. De hierbij gevonden resonantie-frequentie hangt op eenvoudige wijze samen met de natuurlijke ferromagnetische resonantiefrequentie van hetzelfde ferriet. In dit hoofdstuk worden ook meetresultaten gegeven die wijzen op een nieuw relaxatieverschijnsel dat zo niet de enige, dan toch een belangrijke oorzaak is van de restverliezen in ferrieten.

Nadat in hoofdstuk 6 een kort overzicht volgt van de in de literatuur bekende dispersie-mechanismen voor verplaatsingen van B l o c h-wanden en gezamenlijke draaiingen van de spins in een W e i s s-gebied, worden in het volgende hoofdstuk de meetresultaten met de theorie vergeleken. Wij komen hierin tot de volgende conclusies:

a. De relaxatie van de irreversible B l o c h-wand-verplaatsingen wordt veroorzaakt door een demping waarvan de oorzaak nog onbekend is.

b. Het denkbeeld van de ferromagnetische resonantie leidt tot een verklaring van vele eigenschappen der aanvangspermeabiliteit van ferrieten bij hoge frequenties.

c. De relaxatie die bij lage frequentie een dispersie veroorzaakt in de aanvangspermeabiliteit van ferrieten hangt samen met een diffusie van electronen. De activeringsenergie van het relaxatieverschijnsel is dezelfde als die van de soortelijke weerstand van het ferriet, als men deze meet met zeer kleine gelijkstromen.

In het laatste hoofdstuk wordt ingegaan op het feit dat hoewel voor sommige ferrieten de irreversibele wandverplaatsingen bij hoge frequentie niet meer voorkomen, een hoogfrequent magnetisch wisselveld in deze stoffen toch nog veel verliezen veroorzaakt. Een gevolg hiervan is dat het in het algemeen niet gerechtvaardigd is bij ferrieten uit de hysteresis-verliezen de vervorming te berekenen.

Dit onderzoek is gedaan in het Natuurkundig Laboratorium van de N.V. Philips' Gloeilampenfabrieken te Eindhoven. Bij het tot stand komen van het proefschrift gaat mijn dank vooral uit naar de Directie van dit laboratorium voor het vertrouwen dat zij in mij heeft gesteld en voor de wijze waarop zij voortdurend de meetmethodes en de meetresultaten met mij heeft besproken. Dit werk is slechts tot stand kunnen komen door de ongelimiteerde medewerking van vrienden en collegae in het laboratorium. Ik prijs mij gelukkig dat ik in staat ben gesteld een deel van het werk van Dr J. L. Snoek te mogen voortzetten onder leiding van Dr J. J. Went, die dagelijks een daadwerkelijke steun voor mij was. Prof. Dr G. W. Rathenau en Ir J. Smit ben ik veel dank verschuldigd voor de uitgebreide discussies die we naar aanleiding van de meetresultaten mochten hebben, en waaruit vaak suggesties voor nieuwe proeven ontstonden. De heer H. van der Heide is zeer behulpzaam geweest bij het verkrijgen van een aantal van de meetresultaten.

REFERENCES

1. Bragg, W. H. Nature *95*, 561 (1915) and Phil. Mag. *30*, 305 (1915).
2. Barth, T. F. W. and Posnjak, E. Z. Kristallogr. *82*, 325 (1932).
3. Verwey, E. J. W. and Heilmann, E. L. J. chem. Phys. *15*, 174 (1947).
4. Bertaut, F. J. Phys. Radium *12*, 252 (1951).
5. Néel, L. Ann. Phys., Paris *3*, 137 (1948).
6. Kramers, H. A. Physica *1*, 182 (1934).
7. Anderson, P. W. Phys. Rev. *79*, 350 (1950) and *79*, 705 (1950).
8. Néel, L. C. R. Acad. Sci. *230*, 190 (1950).
9. Gorter, E. W. Nature *165*, 798 (1950) and C. R. Acad. Sci. *230*, 192 (1950).
10. Guillaud, Ch. J. Phys. Radium *12*, 239 (1951).
11. Shull, C. G., Wollan, E. O. and Koehler, W. C. Phys. Rev. *84*, 912 (1951).
12. Hastings, J. M. and Corliss, L. M. Rev. mod. Phys. January 1953.
13. Snoek, J. L. "New Developments in Ferromagnetic Materials", Elsevier, Amsterdam—New York 1947.
14. De Boer, J. H. and Verwey, E. J. W. Proc. phys. Soc. (A) *59*, 59 (1937).
15. Verwey, E. J. W., Haayman, P. W., Romeyn, F. C. and van Oosterhout, G. W. Philips Res. Rep. *5*, 173 (1950).
16. van der Burgt, C. M., Gevers, M. and Wijn, H. P. J. Philips techn. Rev. *14*, (1952).
17. Gumlich, E. "Leitfaden der magnetischen Messungen", Vieweg, Braunschweig, 1918.
18. Heisenberg, W. Z. Phys. *69*, 287 (1931).
19. Bloch, F. Z. Phys. *74*, 295 (1932).
20. Bitter, F. Phys. Rev. *38*, 1903 (1931).
21. Williams, H. J., Bozorth, R. M. and Shockley, W. Phys. Rev. *75*, 155 (1949).
22. Bozorth, R. M. "Ferromagnetism" van Nostrand Co, New York, 1951, p. 476.
23. Kersten, M. "Grundlagen einer Theorie der Ferromagnetischen Hysterese und Koerzitivkraft". Hirzel, Leipzig, 1943.
24. Néel, L. Ann. Univ. Grenoble *22*, 299 (1946) and Physica *15*, 225 (1949).
25. Guillaud, Ch. J. Phys. Radium *12*, 239 (1951).
26. Peterson, E. Bell Syst. techn. J. *7*, 762 (1928).
27. Jordan, H. Elekt. Nachr. Tech. *1*, 7 (1924).
28. Legg, V. E. Bell Syst. techn. J. *15*, 39 (1936).
29. Becker, R. Phys. Z. *33*, 905 (1932).
30. Bozorth, R. M. Rev. mod. Phys. January issue 1953.

31. Feldtkeller, R. Fernmeldetech. Z. *3*, 112 (1950) and "Soft Magnetic Materials for Telecommunications" Pergamon Press, London 1953.
32. Williams, H. J., Shockley, W. and Kittel, C. Phys. Rev. *80*, 1090 (1950).
33. Snoek, J. L. and Beljers, H. G. Philips techn. Rev. *11*, 313 (1949).
34. Brockman, F. G., Dowling, P. H. and Steneck, W. G. Phys. Rev. *77*, 85 (1950).
35. Kronig, R. J. opt. Soc. Amer. *12*, 547 (1926).
Kramers, H. A. "Atti Congr. Fisici", Como, 1927 p. 545.
36. Beljers, H. G., van der Lindt, W. J. and Went, J. J. J. appl. Phys. *22*, 1506 (1951).
37. Becker, R. and Kersten, M. Z. Phys. *64*, 664 (1930).
38. Domenicali, C. A. Phys. Rev. *78*, 458 (1950).
39. Becker, R. and Döring, W. "Ferromagnetismus" Springer, Berlin, 1939, p. 105.
40. Döring, W. Z. Naturf. *3a*, 373 (1948).
41. Landau L. and Lifshitz, E. Phys. Z. Sowjet. *8*, 153 (1935).
42. Becker, R. J. Phys. Radium *12*, 332 (1951).
43. Rado, G. T. Phys. Rev. *83*, 821 (1951).
44. Kittel, C. Phys. Rev. *80*, 918 (1950) and J. Phys. Radium *12*, 291 (1951).
45. Becker, R. Phys. Z. *39*, 856 (1938).
46. Néel, L. J. Phys. Radium *5*, 265 (1944).
47. Griffiths, J. H. E. Nature *158*, 670 (1946).
48. Kittel, C. Phys. Rev. *73*, 155 (1948).
49. van Vleck, J. H. Phys. Rev. *78*, 266 (1950).
50. Polder, D. Phil. Mag. *40*, 99 (1949).
51. Snoek, J. L. Nature *160*, 90 (1947).
52. Polder, D. Remark, J. Phys. Radium *12*, 337 (1951).
53. Polder, D. and Smit, J. Rev. mod. Phys. January issue 1953.
54. Galt, J. K. Phys. Rev. *85*, 664 (1952).
55. Yager, W. A., Galt, J. K., Merritt, F. R. and Wood, E. A. Phys. Rev. *80*, 744 (1950).
56. Galt, J. K., Matthias, B. T. and Remeika J. P. Phys. Rev. *79*, 391 (1950).
57. Galt, J. K., Yager, W. A., Remeika, J. P. and Merritt, F. R. Phys. Rev. *81*, 470 (1951).
58. Rado, G. T., Wright, R. W. and Emerson, W. H. Phys. Rev. *80*, 273 (1950).
59. Verwey, E. J. W. and Haayman, P. W. Physica *8*, 979 (1941).
60. Verwey, E. J. W., Haayman, P. W. and Romeyn F. C. J. chem. Phys. *15*, 181 (1947).
61. Richter, G. Ann. Phys. Lpz. *29*, 605 (1937).
62. Schulze, H. "Probleme der Technischen Magnetisierungskurven" Springer, Berlin, 1938, p. 114.
63. Snoek, J. L. Physica *8*, 711 (1941).

STELLINGEN

I

De dispersie welke bij hoge frequenties optreedt in de aanvangspermeabiliteit van polykristallijne gesinterde nikkel-zink-ferrieten is het gevolg van een resonantieproces zoals aangegeven door Snoek, en niet van een relaxatieproces zoals Fomenko en anderen ten onrechte veronderstellen.

Snoek, J. L., Physica *14*, 207 (1948).
Fomenko, L. A., J. exp. theor. Phys. *21*, 1201 (1951).
Wijn, H. P. J., v. d. Burgt, C. M. en Gevers, M., Rev. mod. Phys., January issue 1953.
Dit proefschrift Hfdst. 5. 2.

II

Bij de ferrieten wordt een belangrijk deel van de restverliezen bij lage frequentie veroorzaakt door een relaxatieproces voor electronen.

Wijn, H. P. J. en v. d. Heide, H., Rev. mod. Phys., January issue 1953.
Dit proefschrift Hfdst. 5. 3.

III

De hysteresisweerstand die voor ferromagnetische stoffen in het Rayleigh-gebied wordt gedefinieerd, is bij de ferrieten geen maat voor de niet-lineariteit welke zij in circuits veroorzaken. Het is daarom onjuist bij deze stoffen de kwaliteitsfactoren q_g, a, c_h of h als maat voor de vervorming te gebruiken.

Wijn, H. P. J., „Soft Magnetic Materials for Telecommunications" Pergamon Press, London (1953).
Dit proefschrift Hfdst. 8. 4.

IV

De methode waarbij uit de eigenschappen van de staande golven van een gedeeltelijk met een vaste stof gevulde golfpijp, de complexe waarden van de diëlectrische constante en magnetische permeabiliteit van deze stof wordt bepaald, is gelijkwaardig aan

de methode waarbij dit geschiedt in een trilholte welke gedeeltelijk met de te onderzoeken stof is gevuld.

V

Het probleem van de systematische fout in de helling van de regressie-lijn welke is bepaald volgens de methode der kleinste kwadraten, wordt door de bepaling van de regressie-lijn volgens de zogenaamde parametervrije methode, niet afdoende opgelost.

Lit. Theil, H., Statistica *5*, 97 (1951).

VI

Met behulp van het dualiteits-beginsel van Wallace en Raisbeck kan men schakelingen waarin radiobuizen voorkomen, omvormen in schakelingen waarin punt-contact-transistoren worden toegepast, dit leidt echter in vele gevallen niet tot de gunstigste resultaten. Principiële bezwaren kunnen ook worden aangevoerd.

Wallace, R. L. en Raisbeck, G., Bell Syst. techn. J. *30*, 381 (1951).

VII

In tegenstelling met het tot nu toe in de literatuur vermelde, moet bij de radiologische vergrotingstechniek niet zo zeer de geometrische vergroting dan wel de hierbij bereikte contrastverbetering als belangrijkste winstfactor worden aangemerkt.

VIII

De zuurstofdruk waarmee stoechiometrisch magnetiet bij haar smeltpunt in evenwicht is, is aanmerkelijk lager dan de door Darken en Gurry opgegeven waarde.

Darken, L. S. en Gurry, R. W., J. Am. Chem. Soc. *72*, 3906 (1950).
Wijn, H. P. J., Nature *170*, 707 (1952).

IX

De door Charles gegeven dimensionering van het weerstandsnetwerk ter bepaling van potentiaal-verdelingen met omwentelingssymmetrie, is onjuist voor de as. Dit kan eenvoudig verbeterd worden.

Charles, D., Ann. d. Radioélectricité, *4*, 33 (1949).

X

Het feit dat alkalihalogeniden en andere verbindingen van alkali- en aardalkalimetalen een secundaire electronenemissie-coëfficiënt hebben die de waarde één ver overschrijdt, behoeft niet noodzakelijk verklaard te worden door de aanwezigheid van positieve ladingen aan het oppervlak, een opvatting die met name door Russische onderzoekers naar voren wordt gebracht. Er zijn evenwel gevallen waarbij de aanwezigheid van een positieve oppervlaktelading een essentiële rol speelt.

Trey, F., Phys. Zs. *44*, 38 (1942).

XI

In vele voor de Middelbare Scholen bestemde leerboeken welke handelen over de Natuurkunde, wordt de titel „Magnetisme" gebruikt voor het hoofdstuk dat handelt over ferromagnetische verschijnselen. Dit is misleidend.

XII

Vanuit het standpunt van de onderzoeker in een laboratorium gezien, behoeft de Octrooiwet in Nederland een zodanige wijziging, dat rechtstreekse octrooibescherming voor stoffen niet langer is uitgesloten. In het algemeen is het heden ten dage inconsequent dat de Octrooiwet wel bescherming kent voor nieuwe voorwerpen en niet voor nieuwe stoffen.

XIII

Indien industrialisatie voor Nederland noodzakelijk is, dan vormt de achteruitgang van het aantal ingeschreven studenten aan de Technische Hogeschool te Delft een klemmend argument voor de stichting van een tweede technische hogeschool in Nederland.

H. P. J. Wijn. 28—1—1953.